Critical concentration of formate governs the expression of the flagellar and the pathogenicity island-1 genes in *Salmonella* Typhimurium

Debapriya Mukherjee[1], Dipshikha Chakravortty[1,2*]

[1]Department of Microbiology and Cell Biology, Division of Biological Sciences, Indian Institute of Science, Bangalore, India.

[2]School of Biology, Indian Institute of Science Education and Research, Thiruvananthapuram, 695551.

[*]Corresponding author: dipa@iisc.ac.in

Tel: 0091 80 2293 2842

Fax: 0091 80 2360 2697

Summary

Salmonella enterica is a Gram-negative foodborne pathogen belonging to the family *Enterobacteriaceae* that accounts for global disease burden and has become a top priority pathogen. The stealthy pathogen *Salmonella* can sense diverse cues from the host and modify the expression of its virulence factors. Formate is one of the important constituents of Short Chain Fatty Acids (SCFAs) present in the distal ileum and has previously been studied as an important signal to promote invasion in *Salmonella* Typhimurium. To unravel whether endogenous formate level is also crucial for conferring virulence in *Salmonella*, we have created genomic knockouts of *pflB* (Pyruvate-formate lyase) and *focA* (Formate transporter), the two major contributors to formate pool in *Salmonella*. Perturbing the intracellular pool of formate by deletion of *pflB* resulted in some major reprogramming like the loss of flagella and enhanced expression of pathogenicity island-1 genes. Moreover, STM *ΔpflB* was associated with a higher intracellular pH and membrane damage compared to the WT strain. Our data shows that the membrane damage seen in STM *ΔpflB* leads to the downregulation of the flagellar apparatus mediated by the extra cytoplasmic sigma factor RpoE. Moreover, this same regulon leads to the enhanced expression of pathogenicity island-1 genes, *hilA* and *prgH*. In this study, we show for the first time that endogenous formate levels are of utmost importance to maintain the optimum pH and regulate gene expression in STM. PflB might act as a switch to maintain the optimum cytosolic pH and maximize the virulence of STM under different niches.

Keywords: Short Chain Fatty Acids (SCFAs), Formate, Flagella, Intracellular pH, Membrane depolarization

Introduction

The genus *Salmonella* constitutes of Gram-negative gammaproteobacteria that infects a wide range of human and animal hosts (1). Non-typhoidal serovars like *Salmonella* Typhimurium are commonly associated with self-limiting diarrheal illness with less fatality. The Global Burden of Diseases, Injuries, and Risk Factors Study (GBD) 2017 estimated a total of 95.1 million cases of *Salmonella* enterocolitis with a fatality of 50,771 individuals (2-4). Non-typhoidal infection is mostly limited to the intestine, however, sometimes non-typhoidal serovars can invade the sterile tissues and cause bacteremia, meningitis, and other focal infections. This invasive non-typhoidal infections increase the percentage of case mortalities (5).

Salmonella Typhimurium enters the body of the healthy host via contaminated food and water. One line of defence posed by the host are the Short Chain Fatty Acids (SCFAs) of the small intestine. SCFAs are derived from the anaerobic fermentation of non-digestible polysaccharides, like resistant starches and dietary fibres. The main SCFAs present in the intestine are acetate (C_2), propionate (C_3), and butyrate (C_4) (present in a ratio of 60:20:20) and their concentrations can be as high as 10 to 100 mM. Recent studies have vastly characterized the role of SCFAs in *Salmonella* infection (6-10). Propionate has been seen to diffuse across the cell membrane of STM and the resulting change in the cytoplasmic pH initiated an acid stress response and inhibited bacterial growth (11). Other studies have established the role of butyrate in downregulating the expression of pathogenicity island-1 genes in STM and impair bacterial invasion and translocation from intestine to the bloodstream (12-14). Also, the decreased intracellular pH upon SCFA exposure can slow the flagellar motor and attenuate the motility (15). Moreover, the quorum quenching ability of the organic acids make them a lucrative antimicrobial agent and food preservative (15, 16).

Another member of the SCFAs in the intestine is formate. Previous literature has established the role of formate in acting as a diffusible signal to stimulate the invasion of *Salmonella*

70 Typhimurium (17). It has also been shown that imported and unmetabolized formic acid
71 functions as a cytoplasmic signal that binds to HilD, the master transcriptional regulator of
72 *Salmonella* invasion, and prevents the repressive fatty acids from binding to the same. Thus, it
73 enhances the lifetime of HilD and subsequent derepression of invasion genes (18). Also,
74 formate utilization by the respiratory formate dehydrogenase-N (FdnGHI) and formate
75 dehydrogenase-O (FdoGHI) are instrumental in the gut colonization by *Salmonella*. The
76 formate utilized by STM was produced both by its endogenous enzyme pyruvate-formate lyase
77 (PflB) as well as imported from the intestinal environment (19). However, very few studies
78 have characterized the role of the endogenous formate in controlling the virulence and
79 pathogenesis of *Salmonella* (20). In this study, we were initially trying to characterize the role
80 of endogenously produced formate in the pathogenic lifestyle of STM. In the process, we have
81 uncovered an interesting role of the formate pool in coordinating the expression of the flagellar
82 genes and the SPI-1 genes during the intestinal colonization of *Salmonella* Typhimurium.

83

84

85 Results and discussion

86 Deletion of *pflB* gene leads to decreased percent invasion in Caco-2 cell line and is 87 partially recovered upon supplementation of Sodium Formate

88 To understand the role of formate in *Salmonella* virulence and pathogenesis, we generated
89 knockout strains of *pflB* and *focA* using one-step gene inactivation technique as described
90 previously by Datsenko and Wanner (21). FocA was the formate transporter in *Salmonella*
91 Typhimurium that acts as a passive export channel at high external pH and switches to an active
92 formate importer at low pH (22). Since *focA* and *pflB* genes are in an operon, we proceeded to

93 understand whether deletion of one gene impacted the expression of the other gene (23). We
94 found that deletion of the upstream *focA* gene led to a decreased expression of the downstream
95 gene *pflB* (**Figure S2 B**). However, deletion of *pflB* increased the expression of *focA* gene
96 (**Figure S2 A**). Deletion of either of the genes did not affect the *in-vitro* growth of *Salmonella*
97 in complex LB media, M9 Minimal Media, and there was no observable change upon
98 incubating the strains in M9 Minimal Media supplemented with 40 mM Sodium Formate
99 (referred to as F from henceforth) (**Figure S1**). Similar observations were made for the double
100 knockout strain (**Figure S1**). We proceeded to validate that deletion of *pflB* and *focA* indeed
101 depleted the cell of its indigenous formate pool. For that purpose, we collected the lysate of
102 logarithmic phase cultures of all the strains and quantified the formate concentration by Gas
103 Chromatography Mass Spectrometry (GC-MS). Upon normalization with the CFU, we
104 observed that deletion of *pflB* led to a significant decrease in the intracellular formate
105 concentration. However, deletion of *focA* did not cause a significant change in the normalized
106 intracellular concentration (**Figure 1A**). This raised the possibility of an alternate formate
107 transporter. To test this, we incubated the secondary cultures of all the strains in formate
108 supplemented media and after 3h of incubation, we assayed for the formate concentration in
109 the spent media by GC-MS. Here, we found a significant decrease of the formate concentration
110 in the spent media of STM *ΔfocA* compared to the control, which indicated the presence of an
111 alternate formate importer (**Figure 1B**). Since STM *ΔfocA* retained intracellular formate like
112 STM WT, we focused our study on STM *ΔpflB* where we were able to successfully deplete the
113 formate pool.

114 Intracellular Cell Survival Assay (ICSA) in human colorectal carcinoma cell line Caco-2
115 revealed that STM *ΔpflB* was deficient in percent invasion which was partially recovered upon
116 supplementation of F (**Figure 1C**). The invasion deficiency in the knockout was also recovered
117 upon complementing the gene via an extragenous pQE60 plasmid (**Figure S2 C**). Fold

118 proliferation of STM *ΔpflB* and STM *ΔpflB*+F in Caco-2 was like STM WT (**Figure 1D**).
119 Supplementation of F did not affect the percent invasion of STM WT (**Figure 1C**). However,
120 STM WT supplemented with F had a decreased fold proliferation in Caco-2 (**Figure 1D**). STM
121 *ΔpflB* had a decreased percent phagocytosis in murine macrophage cell line RAW 264.7 which
122 was partially recovered in STM *ΔpflB*+F. Although supplementation of F led to a decreased
123 mean percent phagocytosis for STM WT, we found it to be statistically insignificant (**Figure**
124 **1E**). STM *ΔpflB* was hyperproliferative in RAW 264.7 cell line. STM WT+F also showed a
125 higher fold proliferation compared to STM WT (**Figure 1F**). To confirm whether the invasion
126 deficiency of STM *ΔpflB* was also observed in animal model, we orally gavaged 10^7 CFU of
127 STM WT and STM *ΔpflB* in 6-8 weeks old male C57BL/6 mice. Adhesion deficient STM *ΔfliC*
128 was used as a control. 6h post infection, we found a reduced bacterial burden in mouse intestine
129 for STM *ΔpflB*, which was also associated with an enhanced fecal shedding compared to STM
130 WT (**Figure 1 G, H, I**). These observations were in line with the control STM *ΔfliC* used in
131 this study (**Figure 1 H, I**). Deletion of *fliC* from STM makes it adhesion deficient and leads to
132 its faster clearance from the host body (24).

133

134 **STM *ΔpflB* was deficient in flagella and the deficiency was recovered upon**
135 **supplementation of formate**

136 *Salmonella* Typhimurium uses adhesins like flagella to adhere to host cells during infection
137 (25-27). Following successful adhesion, it uses *Salmonella* Pathogenicity Island-1 (SPI-1)
138 arsenals to invade non-phagocytic epithelial cells (28-30). Our previous data showed that STM
139 *ΔpflB* is deficient in percent invasion in Caco-2 cell line with partial recovery upon
140 supplementation of formate. Quite interestingly, we found that STM *ΔpflB* had a higher
141 expression of *prgH*, which encodes the apparatus protein of SPI-1. The expression was further

142 enhanced in STM *ΔpflB*+F. Alongside, STM WT+F had a significantly higher expression of
143 *prgH* compared to STM WT (**Figure 2A**). This data was in line with the findings of Huang *et*
144 *al* (17). Interestingly we found that STM *ΔpflB* had a reduced expression of *fliC* with a
145 significant recovery in +F conditions. Formate supplementation also reduced the expression of
146 *fliC* in STM WT compared to untreated control (**Figure 2B**). The flagella deficiency of STM
147 *ΔpflB* was confirmed by Transmission Electron Microscopy (TEM). We also found that the
148 flagellar apparatus was intact in the formate transporter *focA* knockout (**Figure 2C**). The
149 quantification of normalized MFI in confocal microscopy and the adhesion assay performed in
150 Caco-2 cell line validated the flagella deficiency upon depleting the cell off its formate pool
151 (**Figure 2D, E, F**). As expected, STM *ΔfocAΔpflB* was also deficient in flagella with a
152 subsequent recovery when incubated in presence of F. (**Figure S3 A, B, C**). These data
153 indicated that the flagellar expression is driven by the end-product formate and not the enzyme
154 PflB.

155 Further, we incubated the secondary cultures of STM WT and STM *ΔpflB* in variable
156 concentrations of formate. Quite interestingly, we found that formate can significantly inhibit
157 the expression of *fliC* starting from a concentration of 1 mM. However, a concentration of
158 0.125 mM was sufficient to significantly recover the attenuated *fliC* expression in STM *ΔpflB*
159 (**Figure S5 A**). 10 mM formate was able to significantly upregulate the expression of *hilA,* the
160 master regulator of SPI-1, in both the strains (**Figure S5 B**).

161 To understand the specificity of formate in controlling this phenomenon, we incubated the
162 secondary cultures of STM WT and STM *ΔpflB* with 40 mM of acetate, propionate, and
163 butyrate. We found that observations with acetate supplementation were in line with the ones
164 obtained upon F supplementation (**Figure S6 B**). This can be explained by the fact that pyruvate
165 is hydrolyzed into formate and acetyl CoA by the PflB enzyme. A part of this acetyl CoA can
166 be converted to acetate (23, 31). This shows that PflB enzyme can regulate the flagella

167 synthesis machinery by maintaining the pool of its end products formate and acetyl CoA. In
168 STM WT, where the *pflB* gene is intact, formate and acetate downregulate *fliC* expression,
169 showing that critical concentration of both the metabolites are important in regulating flagellar
170 expression and the phenomenon is independent of the PflB enzyme.

171

172 **STM *ΔpflB* caused attenuated infection in *in-vivo* mouse model when introduced via the**
173 **oral route**

174 To further understand the role of *pflB* in STM pathogenesis, we extended our study to the *in-*
175 *vivo* mouse model. We orally gavaged 10^7 CFU of bacteria in 6-8 weeks old male C57BL/6
176 mice and euthanized the mice 5 days post infection (dpi) to determine the bacterial burden in
177 the liver, the spleen, and the brain (**Figure 2G, H**). We found a significantly reduced bacterial
178 burden in the liver and the spleen when infected with STM *ΔpflB* as compared to infection with
179 STM WT (**Figure 2G, H**). We also found that C57BL/6 mice infected with STM *ΔpflB* had a
180 better survival rate as compared to mice infected with STM WT (**Figure 2I**). In line with our
181 previous findings, we observed that oral gavaging of STM *ΔfocA* led to similar bacterial burden
182 in the liver and the spleen as STM WT 5dpi. STM *ΔfocAΔpflB* showed lesser organ burden in
183 the liver and spleen of C57 mice model (**Figure S3 D, E**).

184 We subjected C57BL/6 mice to an intra-peritoneal infection with 10^3 CFU of both the WT and
185 the knockout strains. Under these conditions, we observed no significant change in the organ
186 burden of STM WT and STM *ΔpflB* 3dpi (**Figure S4A, B, C, D**). All these data suggested that
187 the reduced organ burden of STM *ΔpflB* upon oral gavaging is due to its attenuated adhesion
188 in the gastrointestinal tract, which promoted a faster clearance from the host body.

189

190 **STM *ΔpflB* had a higher intracellular pH and higher membrane depolarization, both of**
191 **which were recovered upon formate supplementation**

192 Previous studies in *Escherichia coli* had suggested that formate translocation across the FocA
193 channel and metabolism via the FHL-1 (Formate Hydrogen Lyase-1) Complex plays an
194 important role in maintaining the pH homeostasis of the cell during anaerobic growth or
195 fermentation (31-37). This led us to think whether formate synthesis during aerobic growth of
196 *Salmonella* Typhimurium can also play a role in maintaining the intracellular pH (ipH). Also,
197 weak acids like acetate and benzoate cross through the cell membrane in neutral form, and
198 thereby dissociate to lower the ipH (38). From this, we can also expect the endogenous acetate
199 pool to have a role in maintaining the ipH. To determine the change of intracellular pH with
200 the alteration of pH in the surrounding media, we incubated STM WT and STM *ΔpflB* (+/- F)
201 in phosphate buffers of pH 5.5, 6, and 7. Post incubation, a pH-sensitive dye BCECF-AM was
202 used to stain the cells. A higher 488/405 nm ratio for STM *ΔpflB* at all the pH conditions
203 suggested a higher ipH of the knockout strain with respect to the WT strain. More importantly,
204 F and acetate supplementation helped to reduce the higher ipH in STM *ΔpflB* but did not have
205 any role in altering the ipH of STM WT in all the pH conditions tested (**Figure 3A, Figure S6**
206 **C, D**). To further validate this data, we had transformed STM WT and STM *ΔpflB* with the
207 plasmid pBAD-pHuji that encodes pH sensitive red fluorescent protein. The higher ipH in STM
208 *ΔpflB*/pBAD-pHuji showed that *pflB* plays an important role in maintaining the cytosolic pH
209 in *Salmonella* Typhimurium. As observed post BCECF-AM staining, F did not have any effect
210 on the ipH of STM WT/pBAD-pHuji (**Figure 3B**). This data opens the possibility that
211 extracellular and intracellular formate pool might regulate the expression of *fliC* and *hilA* by
212 independent mechanisms.

213 Disrupted pH homeostasis is one of the reasons behind membrane depolarization in biological
214 systems (39). Therefore, we decided to look at the membrane potential of all the strains with

215 or without F supplementation. Exponential culture of STM *ΔpflB* in LB showed a higher
216 $DiBAC_4$ positive population corresponding to higher membrane depolarization. F
217 supplementation in STM *ΔpflB* successfully reduced the membrane depolarization. However,
218 F did not have a role in the membrane polarization in STM WT (**Figure 3D, E**). Similar
219 observations were made upon staining the cells with the DNA-binding fluorescent dye
220 bisbenzimide (**Figure 3C**). Further, the extent of membrane depolarization in STM *ΔpflB* was
221 reduced when the stationary phase bacteria was subcultured into acidic F media (pH 5) (**Figure**
222 **3E**). The H^+ ions of F media might act to compensate for the disrupted cytosolic acidification
223 in *pflB* knockout strain and thereby help in reversing the membrane depolarization. From these
224 data, we can conclude that intracellular formate pool plays pivotal role in maintaining the ipH
225 of *Salmonella* Typhimurium and therefore helps in sustaining the polarization of the cell
226 membrane.

227 We wanted to find out whether the higher ipH in *pflB* knockout is responsible for the disrupted
228 synthesis of flagellar apparatus. We found that incubation STM *ΔpflB* in acidic LB medium
229 (pH 6) led to an increase in *fliC* transcript (**Figure S6 A**). Hence, we reached the conclusion
230 that higher ipH is responsible for the downstream effects.

231

232 **STM *ΔpflB* had a higher transcript level of *csrB*, raising the possibility of flagella**
233 **inhibition via the *csr* sRNA system**

234 To understand how formate regulates the flagellar operon, we checked the transcript level of
235 some of the class I (*flhD*), class II (*flgA*, *fliA*), class II (*flgK*, *motA*) genes (**Figure 4A**) (40-48).
236 We found that inhibition of flagellar operon in formate deficient *pflB* knockout strain is initiated
237 from the class I genes or prior to that. Transcription of the *flhDC* promoter is regulated by
238 factors like OmpR, Crp, HdfR, H-NS, QseBC, FliA, LrhA, etc(42, 49-51). One of the vastly

239 studied mechanisms of post-transcriptional regulation of *flhDC* is the one mediated by *csr*
240 system. The Csr system is made up of the RNA-binding protein CsrA and the small regulatory
241 RNAs (sRNAs) *csrB* and *csrC* (52). CsrA is a 61 amino acid long protein that binds mRNA of
242 the target genes and thereby prevents or promotes translation (53). CsrA can bind to the *flhD*
243 transcript and stabilize it from 5`-end directed RNase E cleavage (54). The activity of CsrA
244 protein is antagonized by small regulatory RNAs *csrB* and *csrC*. A single *csrB* RNA molecule
245 can bind up to 18 CsrA molecules, whereas a single *csrC* molecule can bind up to 9 CsrA
246 molecules (55-57). In *S.* Typhimurium, CsrA has been seen to regulate motility, virulence,
247 carbon storage, and secondary metabolism (58, 59). The transcription of *csrB* and *csrC* is
248 controlled by the orthologues of BarA/SirA two component systems (TCS) in *E. coli* and *S.*
249 Typhimurium (60-63).

250 We observed that there was an increase in the *csrB* transcript levels in STM *ΔpflB* that reduced
251 in STM *ΔpflB*+F (**Figure 4B**). Since *csrB* directly interacts with CsrA and prevents the activity
252 of the latter, we decided to clone *csrA* in an extragenous plasmid pQE60 and transform the
253 recombinant plasmid in STM *ΔpflB*. IPTG-mediated overexpression of *csrA* led to a partial
254 recovery of the attenuated expression of *fliC* in STM *ΔpflB* (**Figure 4C**). CsrA is known to bind
255 to *flhD* transcript and stabilize the same. However, an abundance of CsrA molecules in the cell
256 might stabilize the *flhD* transcript to an extent that translation is prevented. This explains why
257 overexpression of *csrA* in STM WT resulted in a reduced expression of *fliC*. This finding was
258 supported by adhesion assay in Caco-2 cell line, where we found that STM *ΔpflB*/p: *csrA* had
259 an improved percent adhesion compared to STM *ΔpflB* (**Figure 4D**). The improvement in
260 flagellar number upon overexpressing *csrA* in STM *ΔpflB* was visualized and quantified by
261 TEM and confocal microscopy as well (**Figure 4E, F, G, H**).

262

263 **The extra cytoplasmic sigma factor RpoE increases the expression of *csrB* and therefore**
264 **restricts the expression of *fliC***

265 In *E. coli*, RpoE (σ^E) is an extra cytoplasmic stress factor that is required for viability and
266 regulating cellular response to membrane stress (64). The membrane bound anti-sigma factor
267 RseA binds to σ^E in conjunction with the periplasmic protein RseB (65, 66). In absence of any
268 envelope stress, the binding of RseA to σ^E prevents the latter from interacting with the RNA
269 polymerase (66-69). Upon envelope stress, the proteolytically unstable RseA is degraded
270 rapidly and releases abundant σ^E molecules in the cellular to mediate its downstream functions
271 like activation of gene products involved in biogenesis, transport, and/or assembly of
272 lipopolysaccharides (LPS), phospholipids, and outer membrane proteins (OMPs) that
273 constitute the outer membrane (OM), and the proteases and chaperones that maintain or repair
274 the OM integrity (66). Recent studies have shown that σ^E also activates the transcription of
275 *csrB*/*C* sRNAs indirectly from σ^{70} promoters (70, 71). These studies have been performed in
276 *E. coli*. Deletion of *rpoE* from STM showed the reduction in transcription level of *csrB*
277 (~0.588). This indicated that a similar mechanism might be functional in STM as well (**Figure**
278 **5A**).

279 In our previous data, we had shown that formate produced by PflB maintains the ipH of the
280 cell. Therefore, deletion of the gene perturbs the ipH and leads to membrane depolarization.
281 We hypothesized that the membrane stress in STM *ΔpflB* can lead to the degradation of RseA
282 and the free σ^E can promote the transcription of *csrB*. Our data showed that the enhanced *csrB*
283 expression in STM *ΔpflB* was reduced multiple folds in STM *ΔpflBΔrpoE* (**Figure 5A**). We
284 also found that the low expression of *flhD* and *fliC* in STM *ΔpflB* was reversed in STM
285 *ΔpflBΔrpoE* (**Figure 5B**). This reversal of flagella deficiency further reflected in the improved
286 percent adhesion of STM *ΔpflBΔrpoE* as compared to STM *ΔpflB* in Caco-2 cell line (**Figure**

287 **5C**). TEM and confocal microscopy further confirmed this observation (**Figure 5D, E, F, G**).
288 Thus, we could understand that the attenuated flagella synthesis in STM *ΔpflB* was mediated
289 via the extra cytoplasmic stress factor σ^E.

290

291 **Formate maintains the switch between the flagellar expression and SPI-1 gene expression**
292 **in intestine of the C57BL/6**

293 In our previous data, we had shown that STM *ΔpflB* shown a higher abundance of *prgH*
294 transcript. We wanted to see if this enhanced expression of SPI-1 gene was regulated by this
295 same loop. Hence, we studied the transcript level of *hilA* and *prgH* genes of SPI-1. We found
296 that the increased expression of *hilA* and *prgH* in STM *ΔpflB* was reduced in STM *ΔpflBΔrpoE*
297 (**Figure 6A**). This proved that the intracellular formate regulates the switch from flagellar
298 expression to SPI-1 gene expression.

299 Previous results in our study had shown that F supplementation enhances the expression of
300 *prgH* in STM WT and STM *ΔpflB* (**Figure 2A**). Flagellar motility and invasion in epithelial
301 cells are controlled by the BarA/SirA Two-component system (TCS) (62). As expected, STM
302 *ΔsirA* had a low level of *hilA* and *prgH* expression and F supplementation in STM *ΔsirA*
303 produced no significant change in the expression of the two genes. Deletion of *sirA* in STM
304 *ΔpflB* abolished any significant upregulation in *hilA* and *prgH* levels upon F supplementation
305 (**Figure 6B**). This shows that the extracellular formate influences the virulence and
306 pathogenesis of *Salmonella* via the BarA/SirA TCS. Interestingly, we observed that STM
307 *ΔpflBΔsirA* continued to show a recovery in the *fliC* transcript level under F supplementation.
308 This proves that intracellular formate regulates the pathogenesis of *Salmonella* independent of
309 the BarA/SirA TCS (**Figure 6C**). Hence, if the intracellular pool of formate is maintained by
310 *pflB* gene, extracellular formate influences the expression of the SPI-1 genes via the BarA/SirA

311 TCS. However, if the intracellular pool of formate is perturbed, the resulting membrane damage
312 promotes the RpoE mediated overexpression of *csrB*, associated with decrease in *fliC* transcript
313 level and enhanced *hilA prgH* expression.

314 To understand the physiological relevance of this phenomenon, we studied the expression
315 levels of *pflB* in different parts of the intestine as flagella and SPI-1 are highly instrumental in
316 the intestinal phase of *Salmonella* infection. We found that *pflB* expression reduced from
317 duodenum to the ileum (**Figure 6D**). This led us to hypothesize that *Salmonella* downregulates
318 its *pflB* gene as it approaches its site of invasion- the distal ileum. Downregulation of *pflB* gene
319 can create a partial deficiency of formate in the bacterial cell, eliciting in a membrane
320 depolarization effect, thereby promoting the activity of σ^E, enhancing the abundance of *csrB*
321 molecules, and downregulating the transcription of flagellar operon with the upregulation of
322 the expression of SPI-1 gene cascade. We performed obtained sections of duodenum and ileum
323 from mice infected with STM WT and STM *ΔpflB* and stained with anti-SipC antibody to
324 determine the levels of the SPI-1 effector protein (**Figure 6F**). We further normalized the
325 fluorescence from secondary antibody specific for Rabbit-generated Anti-SipC antibody with
326 the mCherry fluorescence of the bacteria, transformed with pFPV: *mCherry*. We found that the
327 normalized MFI increased from duodenum to ileum for the STM WT infected mice. Whereas
328 there was a decrease in the normalized MFI from duodenum to ileum in the STM *ΔpflB* infected
329 mice (**Figure 6E**). These data show that indeed the formate pool maintained by PflB enzyme
330 negatively regulates the expression of SPI-1 genes and depletion of the former can be a strategy
331 for *Salmonella* Typhimurium to maximize the expression of the latter in the ileum.

332

333 **Conclusion**

334 *Salmonella* harbours a cascade of genes and regulatory factors that maintains the switch
335 between the different aspects of its extracellular and intracellular lifestyle (72). Multiple studies
336 in *Salmonella* Typhimurium have affirmed the regulatory overlap between the flagellar
337 secretion system and the SPI-1. The flagellar protein FliZ is known to post-translationally
338 activate the master regulator of flagella synthesis, i.e.., FlhD. Kage *et al* have shown that FliZ
339 can also regulate HilD, one of the regulators of SPI-1, at the transcriptional level (73, 74). HilD
340 has been found to directly bind to the promoter region of *flhDC* upstream of the P5
341 transcriptional start site and activate its expression (75). Other studies have shown that the
342 expression of SPI-1 can negatively influence the expression of flagellar genes, and this
343 facilitates the pathogenicity and virulence of *Salmonella*. A *fliZ* mutation decreased the
344 expression of *hilA* by 2-fold, whereas *sirA* knockout showed decreased the expression of *hilA*
345 by 10-fold and increased expression of flagella by 100-fold (76-79). Moreover, a latest study
346 by Saleh *et al* have shown that HilD activation can trigger a SPI-1 dependent induction of the
347 stringent response and considerable decrease in the Proton Motive Force (PMF). Although
348 flagellation was unaffected, HilD-induction produced motility defect in *S*. Typhimurium (80).
349 All these studies have shown that *Salmonella* can modulate between its flagella synthesis and
350 SPI-1 gene expression to achieve efficient adhesion and delivery of SPI-1 effectors. There can
351 be multiple advantages of downregulating flagella and upregulating the expression of SPI-1
352 genes. Firstly, downregulation of flagella will prevent the bacteria from swimming away from
353 a cell primed for invasion. Secondly, the flagellar apparatus is immunogenic and
354 downregulating the flagella can be a strategy to subvert the host's immune responses (81-83).
355 Thirdly, simultaneous production of the two apparatus might lead to an interference between
356 the both and manifest itself as misappropriate secretion of flagellin and the SPI-1 effectors (84).

357 In our study, we have knocked out the gene encoding pyruvate-formate lyase enzyme and hence
358 were successful to deplete the cell off its native formate pool. Although the knockout strain did

359 show an enhanced expression of SPI-1 gene *prgH*, it had a reduction in the transcript level of
360 *fliC*. This reflected in an attenuated invasion as well as adhesion in the human epithelial cell
361 line. The deficiencies were partially recovered with the supplementation of 40 mM F. This also
362 explains why it was hyperproliferative in the RAW 264.7 macrophage cell line (85). We have
363 also found that STM *ΔpflB* was unable to maintain its intracellular pH to as par STM WT,
364 which elicited in a membrane depolarization phenotype. Perturbations in the membrane
365 degraded RseA and caused the sigma factor RpoE to enhance the expression of *csrB*. Since
366 *csrB* is known to bind and inhibit CsrA protein, we speculated that the enhanced *csrB* transcript
367 level resulted in a reduced *fliC* expression. Overexpression of *csrA* via an extragenous plasmid
368 led to a partial recovery in the expression of *fliC* and this supported our speculation. Moreover,
369 deletion of *rpoE* in STM *ΔpflB* which could successfully alter the flagella deficient phenotype
370 in the further affirmed our hypothesis. This proved that the extra cytoplasmic sigma factor
371 RpoE was mediating the downstream effects in response to the cell membrane stress.

372 In all our experiments, we had also observed that F supplementation caused a reduced flagellar
373 expression in STM WT. Quite interestingly, supplementation of formate did not influence the
374 intracellular pH or the membrane potential of STM WT. This led us to hypothesize that
375 extracellular formate impacted the pathogenicity of STM differently from intracellular formate
376 synthesis pathway. Huang *et al* have shown that extracellular formate acts as a diffusible signal
377 to promote invasion. However, this was independent of the BarA/SirA Two Component
378 System. Also, they have commented that this was independent of *csrB* that is directly regulated
379 by the action of the response regulator SirA. In our study, we have also found that STM WT+F
380 had a higher expression of SPI-1 genes (17). In contrast with the previous literature, we have
381 found that the *csrB* transcript level was higher in STM WT+F as compared to STM WT. It is
382 highly likely that the elevated *csrB* levels were successfully able to bind to the free CsrA
383 molecules and prevent them from stabilising the *flhD* transcript, thereby bringing about a

384 reduced *fliC* expression. This shows that formate is an essential metabolite of *Salmonella* and
385 critical concentration of formate act to determine whether it will act through the TCS or by
386 regulating the ipH of the cell.

387 *Salmonella* Typhimurium has been vastly studied to alter its metabolism according to the
388 requisites inside the host. For example, butyrate in small intestine promotes the β-oxidation in
389 intestinal epithelial cells, which depletes the oxygen at the epithelial interface (86). During
390 *Salmonella* infection, neutrophils transmigrating to the intestine introduce ROS and RNS, that
391 lead to the generation of tetrathionate and nitrate in the lumen (87, 88). Moreover, inflammation
392 depletes the intestinal lumen off the butyrate-producing bacteria and the intestinal epithelium
393 shifts to lactate fermentation (89). Loss of local oxygen consumption leads to oxygen diffusing
394 in the otherwise anaerobic intestinal lumen (89, 90). *Salmonella* switches to an oxidative
395 central metabolism using oxygen, nitrate, and tetrathionate as terminal electron acceptors and
396 this strategy helps it to efficiently degrade the poorly fermentable sources like the host-derived
397 lactate (91-96). Previously, it has been shown that spatially distinct *Salmonella* populations in
398 the mucous layer and the intestinal lumen vary in their energy metabolism. Transcription of
399 pyruvate-formate lyase and formate dehydrogenases were comparatively higher in the mucous
400 layer as compared to the population in the lumen (19). The study had shown that formate
401 metabolism conferred an enhanced fitness advantage in the mucous layer. In our study we have
402 seen that the transcription of the *pflB* is highest at the large intestine, and it gradually subsides
403 in the small intestine, ie., the site of *Salmonella* infection. It is highly likely that *Salmonella*
404 modulates the expression of *pflB* in response to signals perceived from the local
405 microenvironment of the gut. Thereby, we propose a model of *Salmonella* invasion where it
406 downregulates the *pflB* gene and perturbs the intracellular formate pool once it reaches its site
407 of infection. Therefore, it creates a partial membrane depolarization, which downregulates the
408 flagellar apparatus and promotes the invasion of STM into epithelial cells by induced

expression of the SPI-1 apparatus. The cues and the genetic factors that control this modulation have not been understood. Overall, our study adds up to the knowledge of understanding how intracellular metabolism in *Salmonella* can govern the virulence attributes of the pathogen and reflects upon the possibility of more such interactions for future research.

Acknowledgements

We express our heartfelt gratitude to the financial support from Department of Biotechnology (DBT), Ministry of Science and Technology; Department of Science and Technology (DST), Ministry of Science and Technology. DC acknowledges DAE for the SRC outstanding investigator award and funds, ASTRA Chair Professorship and TATA Innovation fellowship funds. The authors jointly acknowledge the DBT-IISc Partnership Program. Infrastructure support from ICMR (Center for Advanced Study in Molecular Medicine), DST (FIST), and UGC-CAS (special assistance) is acknowledged. DM acknowledges IISc fellowship.

We acknowledge the Departmental Real-Time Facility, Departmental Confocal Microscopy facility, Divisional Electron Microscopy Facility, Divisional Mass Spectrometry Facility, Divisional Flow Cytometry Facility, Central Animal Facility at IISc for providing us opportunity for experimentation. Mr. Sumitlal K and Ms. Navya have helped in image acquisition in Confocal Microscopy. Dr. Sushma and Keerthana helped in image acquisition in Transmission Electron Microscopy. Dr. Muralidhar and Dr. Sunitha helped in formate quantitation studies using Gas Chromatography Mass Spectrometry. Ms. Lipika and Ms. Dhanusha helped in data acquisition from Flow Cytometry. Dr. Akshay Datey is acknowledged for his initial supervision in the study.

Author Contributions

DM and DC have conceived the study and designed the experiments. DM has performed all the experiments and participated in acquiring the data. DM has analysed the data, constructed the figures, and wrote the original draft of the manuscript. DM and DC have participated in the proofreading and editing of the manuscript. DC has supervised the study and helped in fund acquisition. All the authors have read and approved the manuscript.

Declaration of interest

Authors declare no conflict of interest.

Figure Legends

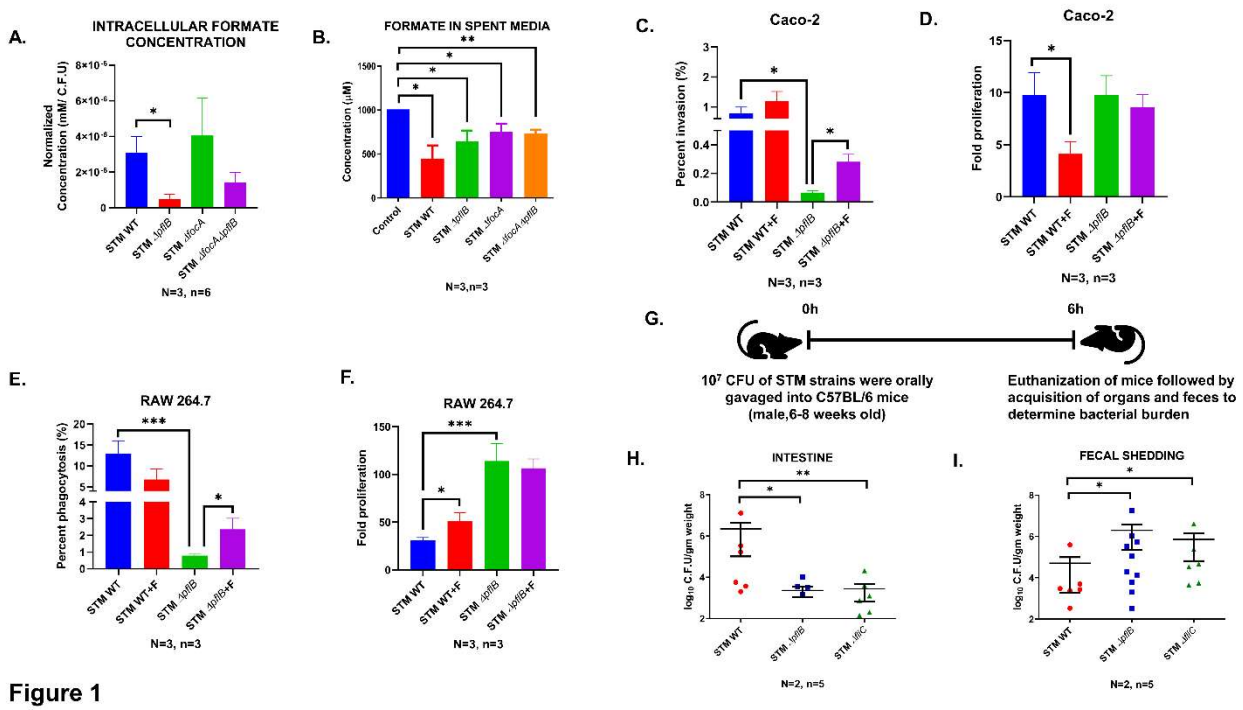

Figure 1

446 **Figure 1: Deletion of *pflB* gene leads to decreased percent invasion in Caco-2 cell line and**
447 **is partially recovered upon supplementation of Sodium Formate**

448 A. GC-MS mediated quantification of intracellular formate in STM WT, STM *ΔpflB*, STM
449 *ΔfocA*, STM *ΔfocAΔpflB*. Data is represented as Mean+/-SEM of N=3, n=6.
450 B. GC-MS mediated quantification of residual formate in the spent media post incubation
451 by STM WT, STM *ΔpflB*, STM *ΔfocA*, STM *ΔfocAΔpflB*. Data is represented as
452 Mean+/-SEM of N=3, n=3.
453 C. Percent invasion of STM WT, STM *ΔpflB* (+/-F) in Caco-2 cell line. Data is represented
454 as Mean+/-SEM of N=3, n=3.
455 D. Fold proliferation of STM WT, STM *ΔpflB* (+/-F) in Caco-2 cell line. Data is
456 represented as Mean+/-SEM of N=3, n=3.
457 E. Percent phagocytosis of STM WT, STM *ΔpflB* (+/-F) in RAW 264.7 cell line. Data is
458 represented as Mean+/-SEM of N=3, n=3.
459 F. Fold proliferation of STM WT, STM *ΔpflB* (+/-F) in RAW 264.7 cell line. Data is
460 represented as Mean+/-SEM of N=3, n=3.
461 G. Schematic showing the protocol followed for invasion assay in C57BL/6 mice
462 H. Bacterial burden in the intestine post 6h of infecting the mice with STM WT and STM
463 *ΔpflB* via oral gavaging. Data is represented as Mean+/-SEM of N=2, n=5.
464 I. Bacterial burden in the feces of mice post 6h of infection with STM WT and STM *ΔpflB*
465 via oral gavaging. Data is represented as Mean+/-SEM of N=2, n=5.

466 (Unpaired Student's t-test for column graphs, Two-way Anova for grouped data, Mann-
467 Whitney U-test for animal experiment data (**** $p < 0.0001$, *** $p < 0.001$, ** $p<0.01$, *
468 $p<0.05$))

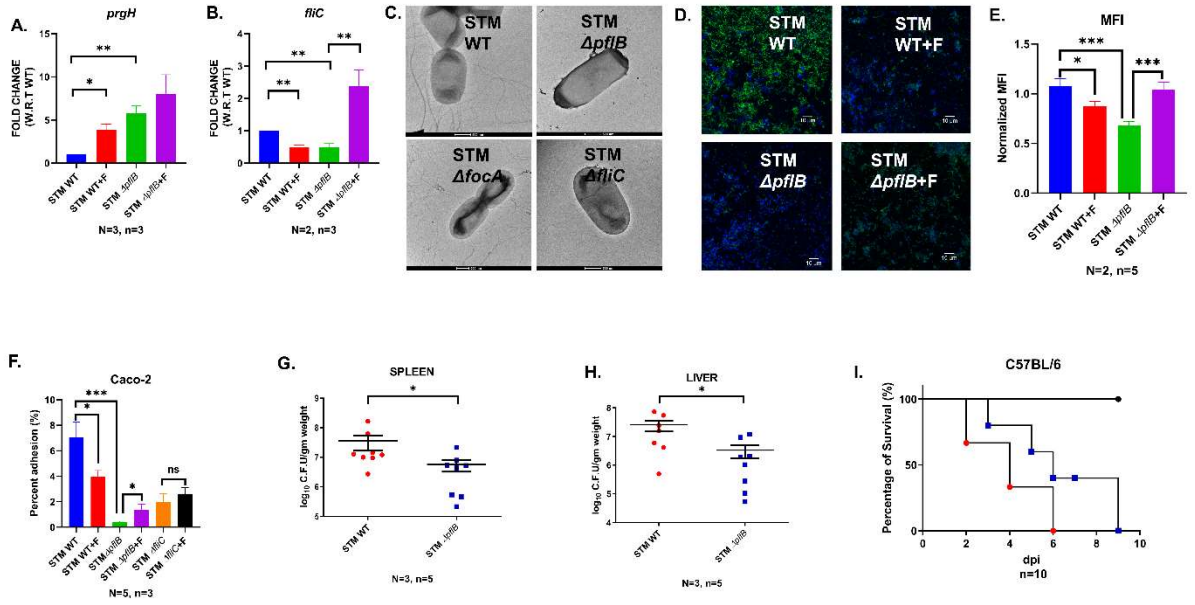

Figure 2

Figure 2: STM *ΔpflB* was deficient in flagella and the deficiency was recovered upon supplementation of formate

A. RT-qPCR mediated study of expression profile of *prgH* in the logarithmic phase cultures of STM WT, STM *ΔpflB* (+/-F). Data is represented as Mean+/-SEM of N=3, n=3.

B. RT-qPCR mediated study of expression profile of *fliC* in the logarithmic phase cultures of STM WT, STM *ΔpflB* (+/-F). Data is represented as Mean+/-SEM of N=2, n=3.

C. TEM assisted visualization of the flagellar structures in STM WT, STM *ΔpflB*, STM *ΔfocA*, STM *ΔfliC*

D. Confocal microscopy assisted visualization of the flagellar structures in STM WT, STM *ΔpflB* (+/-F). Images are representative of N=2, n=5.

E. Normalized Median Fluorescence Intensity (MFI), i.e.., MFI of Secondary antibody for Rabbit generated Anti-fli antibody/ MFI for DAPI in confocal microscopy assisted visualization of the flagellar structures in STM WT, STM *ΔpflB* (+/-F). Data is represented as Mean+/-SEM of N=2, n=5.

F. Percent adhesion of STM WT, STM *ΔpflB*, STM *ΔfliC*(+/-F) in Caco-2 cell line. Data is represented as Mean+/-SEM of N=5, n=3.

G. Organ burden of STM WT and STM *ΔpflB* in spleen 5 days post oral gavaging. Data is represented as Mean+/-SEM of N=3, n=5.

H. Organ burden of STM WT and STM *ΔpflB* in liver 5 days post oral gavaging. Data is represented as Mean+/-SEM of N=3, n=5.

I. Survival rates of C57BL/6 mice post infection with STM WT and STM *ΔpflB* through oral route.

(Unpaired Student's t-test for column graphs, Two-way Anova for grouped data, Mann-Whitney U-test for animal experiment data (**** $p < 0.0001$, *** $p < 0.001$, ** $p<0.01$, * $p<0.05$))

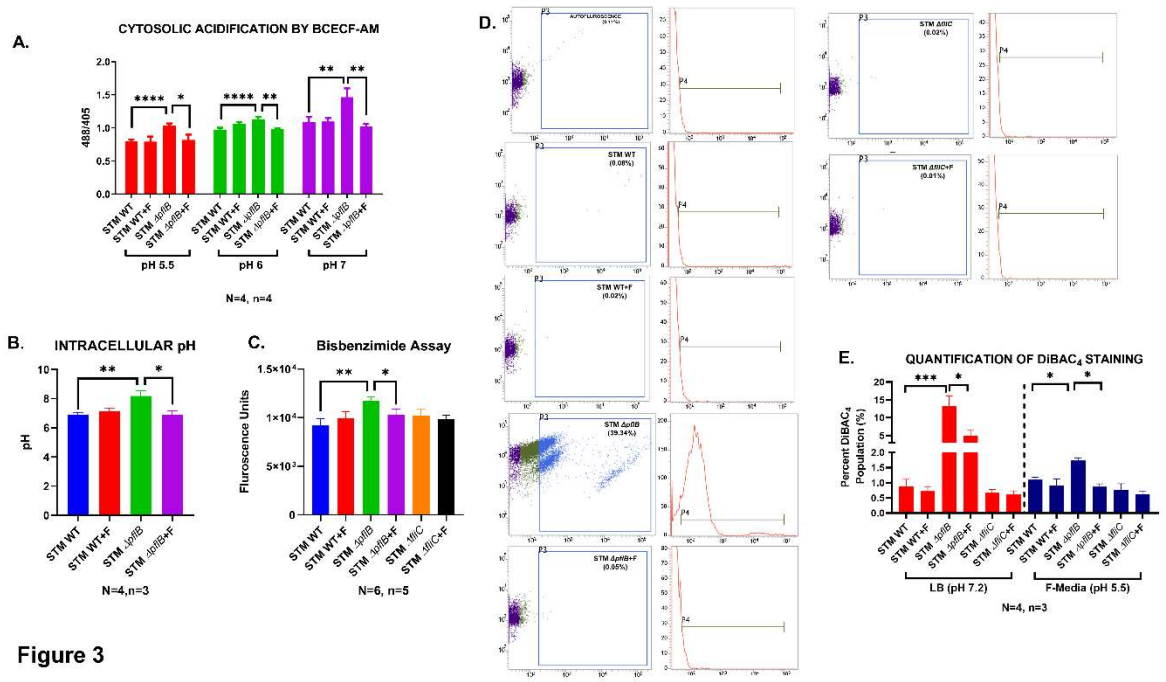

Figure 3

Figure 3: STM *ΔpflB* had a higher intracellular pH and higher membrane depolarization, both of which were recovered upon formate supplementation

500 A. BCECF-AM dye mediated elucidation of the relative ipH in the logarithmic cultures of
501 STM WT, STM *ΔpflB* (+/-F) in phosphate buffers of pH 5.5, 6, and 7. Data is
502 represented as Mean+/-SEM of N=4, n=4.
503 B. Elucidation of the ipH in the logarithmic cultures of STM WT/pBAD-pHuji and STM
504 *ΔpflB*/pBAD-pHuji (+/-F). Data is represented as Mean+/-SEM of N=4, n=3.
505 C. Bisbenzimide assay to quantify the membrane damage in the logarithmic cultures of
506 STM WT, STM *ΔpflB,* STM *ΔfliC* (+/-F). Data is represented as Mean+/-SEM of N=6,
507 n=5.
508 D. Representative FACS percent positive and histogram profiles of $DiBAC_4$ staining in
509 the logarithmic cultures of STM WT, STM *ΔpflB,* STM *ΔfliC* (+/-F). Data is
510 representative of N=4, n=3.
511 E. Flow cytometry obtained quantification of percent- $DiBAC_4$ positive cells in the
512 logarithmic cultures of STM WT, STM *ΔpflB,* STM *ΔfliC* (+/-F) incubated in LB media
513 (pH 7.2) and F-media (pH 5.5). Data is represented as Mean+/-SEM of N=4, n=3.

514 (Unpaired Student's t-test for column graphs, Two-way Anova for grouped data, Mann-
515 Whitney U-test for animal experiment data (**** $p < 0.0001$, *** $p < 0.001$, ** $p<0.01$, *
516 $p<0.05$))

517

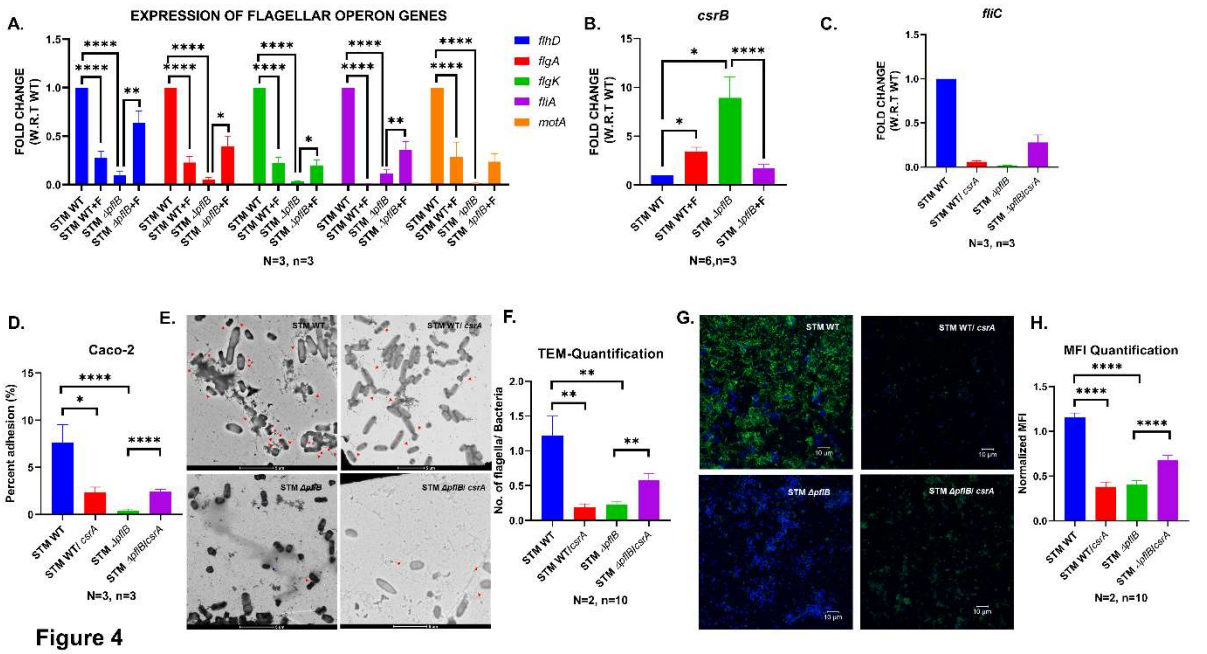

Figure 4

Figure 4: STM *ΔpflB* had a higher transcript level of *csrB*, raising the possibility of flagella inhibition via the *csr* sRNA system

A. RT-qPCR mediated expression profile of the flagellar operon genes *flhD*, *flgA*, *flgK*, *fliA*, *motA* in the logarithmic cultures of STM WT, STM *ΔpflB (+/-F).* Data is represented as Mean+/-SEM of N=3, n=3.

B. RT-qPCR mediated expression profile of the sRNA *csrB* in the logarithmic cultures of STM WT, STM *ΔpflB (+/-F).* Data is represented as Mean+/-SEM of N=6, n=3.

C. RT-qPCR mediated expression profile of the flagellar operon genes *flhD* and *fliC* in the logarithmic cultures of STM WT and STM *ΔpflB* transformed with an pQE60*: csrA* under an IPTG-inducible system. Data is represented as Mean+/-SEM of N=3, n=3.

D. Percent adhesion of STM WT/pQE60: *csrA* and STM *ΔpflB*/pQE60: *csrA* in Caco-2 cell line. Data is represented as Mean+/-SEM of N=3, n=3.

E. TEM assisted visualization of the flagellar structures in STM WT/pQE60: *csrA*, STM *ΔpflB*/pQE60: *csrA.* Data is representative of N=2, n=10.

533 F. Quantification of number of flagella/bacteria in each image obtained by TEM for the
534 logarithmic cultures of STM WT/pQE60: *csrA*, STM *ΔpflB*/pQE60: *csrA*. Data is
535 represented as Mean+/-SEM of N=2, n=10.
536 G. Confocal microscopy assisted visualization of the flagellar structures in STM
537 WT/pQE60: *csrA*, STM *ΔpflB*/pQE60: *csrA*. Images are representative of N=2, n=10.
538 H. Normalized Median Fluorescence Intensity (MFI), i.e.., MFI of Secondary antibody for
539 Rabbit generated Anti-fli antibody/ MFI for DAPI in confocal microscopy assisted
540 visualization of the flagellar structures in STM WT/pQE60: *csrA*, STM *ΔpflB*/pQE60:
541 *csrA*. Data is represented as Mean+/-SEM of N=2, n=10

542 (Unpaired Student's t-test for column graphs, Two-way Anova for grouped data, Mann-
543 Whitney U-test for animal experiment data (**** $p < 0.0001$, *** $p < 0.001$, ** $p<0.01$, *
544 $p<0.05$))

545

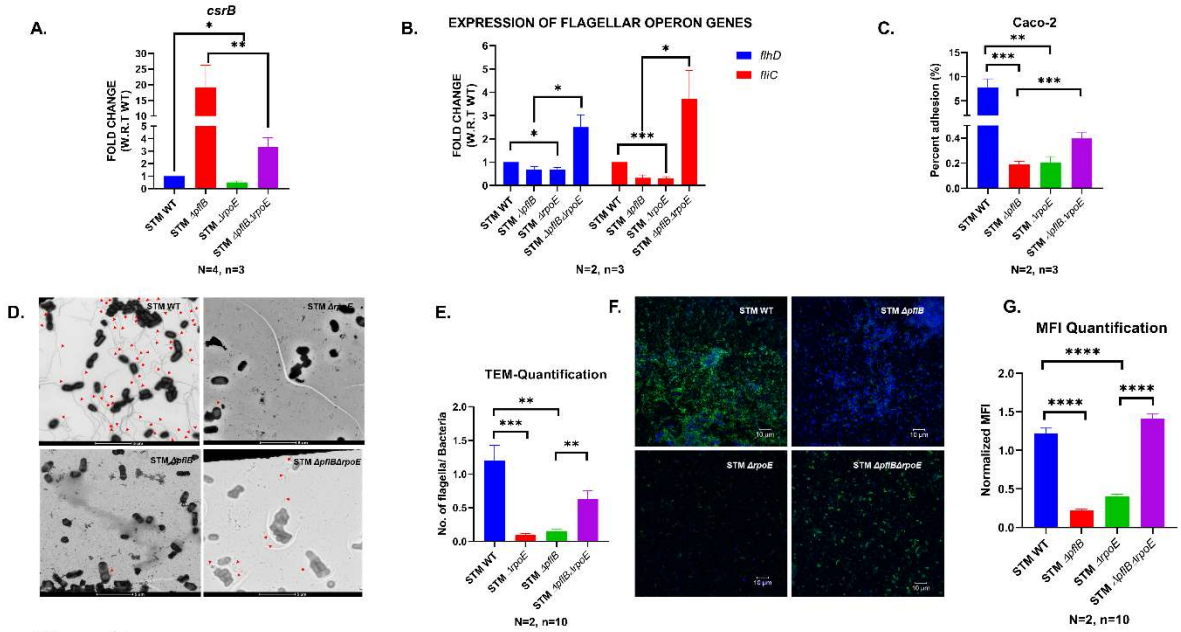

Figure 5

546

547 **Figure 5: The extra cytoplasmic sigma factor RpoE increases the expression of *csrB* and**
548 **therefore restricts the expression of *fliC***

549 A. RT-qPCR mediated expression profile of the sRNA *csrB* in the logarithmic cultures of
550 STM WT, STM *ΔpflB*, STM *ΔrpoE*, STM *ΔpflBΔrpoE.* Data is represented as Mean+/-
551 SEM of N=4, n=3.
552 B. RT-qPCR mediated expression profile of the flagellar operon genes *flhD* and *fliC* in the
553 logarithmic cultures of STM WT, STM *ΔpflB*, STM *ΔrpoE*, STM *ΔpflBΔrpoE*. Data is
554 represented as Mean+/-SEM of N=2, n=3.
555 C. Percent adhesion of STM WT, STM *ΔpflB*, STM *ΔrpoE*, STM *ΔpflBΔrpoE* in Caco-2
556 cell line. Data is represented as Mean+/-SEM of N=2, n=3.
557 D. TEM assisted visualization of the flagellar structures in STM WT, STM *ΔpflB*, STM
558 *ΔrpoE*, STM *ΔpflBΔrpoE.* Data is representative of N=2, n=10.
559 E. Quantification of number of flagella/bacteria in each image obtained by TEM for the
560 logarithmic cultures of STM WT, STM *ΔpflB*, STM *ΔrpoE*, STM *ΔpflBΔrpoE.* Data is
561 represented as Mean+/-SEM of N=2, n=10.
562 F. Confocal microscopy assisted visualization of the flagellar structures in STM WT, STM
563 *ΔpflB*, STM *ΔrpoE*, STM *ΔpflBΔrpoE*. Images are representative of N=2, n=10.
564 G. Normalized Median Fluorescence Intensity (MFI), i.e.., MFI of Secondary antibody for
565 Rabbit generated Anti-fli antibody/ MFI for DAPI in confocal microscopy assisted
566 visualization of the flagellar structures in STM WT, STM *ΔpflB*, STM *ΔrpoE*, STM
567 *ΔpflBΔrpoE*. Data is represented as Mean+/-SEM of N=2, n=10.

568 (Unpaired Student's t-test for column graphs, Two-way Anova for grouped data, Mann-
569 Whitney U-test for animal experiment data (**** $p < 0.0001$, *** $p < 0.001$, ** $p<0.01$, *
570 $p<0.05$))

571

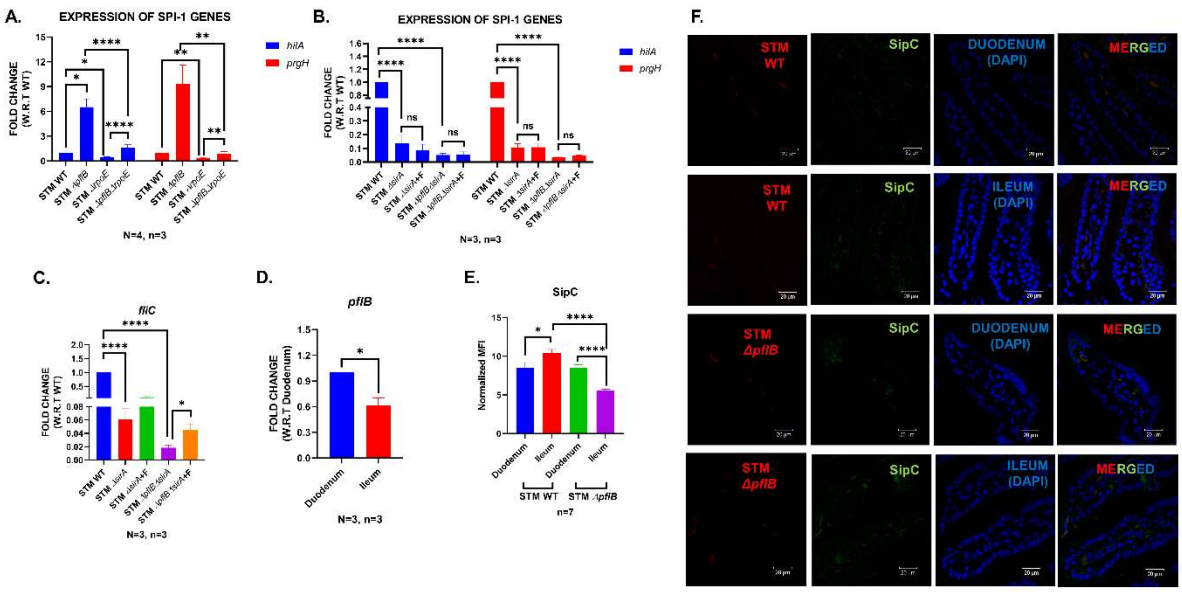

Figure 6

Figure 6: PflB maintains the switch between the flagellar expression and SPI-1 gene expression in intestine of the C57BL/6

A. RT-qPCR mediated expression profile of the SPI-1 genes *hilA* and *prgH* in the logarithmic cultures of STM WT, STM *ΔpflB*, STM *ΔrpoE*, STM *ΔpflBΔrpoE*. Data is represented as Mean+/-SEM of N=4, n=3.

B. RT-qPCR mediated expression profile of *fliC* gene in the logarithmic cultures of STM WT, STM *ΔpflB*, STM *ΔrpoE*, STM *ΔpflBΔrpoE*. Data is represented as Mean+/-SEM of N=3, n=3.

C. RT-qPCR mediated expression profile of *pflB* gene in the duodenum and ileum of the intestine of C57BL/6 mice. Data is represented as Mean+/-SEM of N=3, n=3.

D. Confocal microscopy assisted visualization of the SPI-1 effector SipC protein in the duodenum and ileum of mice infected with STM WT and STM *ΔpflB*. Images are representative of n=7.

E. Normalized Median Fluorescence Intensity (MFI), i.e.., MFI of Secondary antibody for Rabbit generated Anti-SipC antibody/ MFI for mCherry fluorescence from STM

WT/pFPV and STM *ΔpflB/* pFPV in confocal microscopy. Data is represented as Mean+/-SD of n=7.

(Unpaired Student's t-test for column graphs, Two-way Anova for grouped data, Mann-Whitney U-test for animal experiment data (**** $p < 0.0001$, *** $p < 0.001$, ** $p<0.01$, * $p<0.05$))

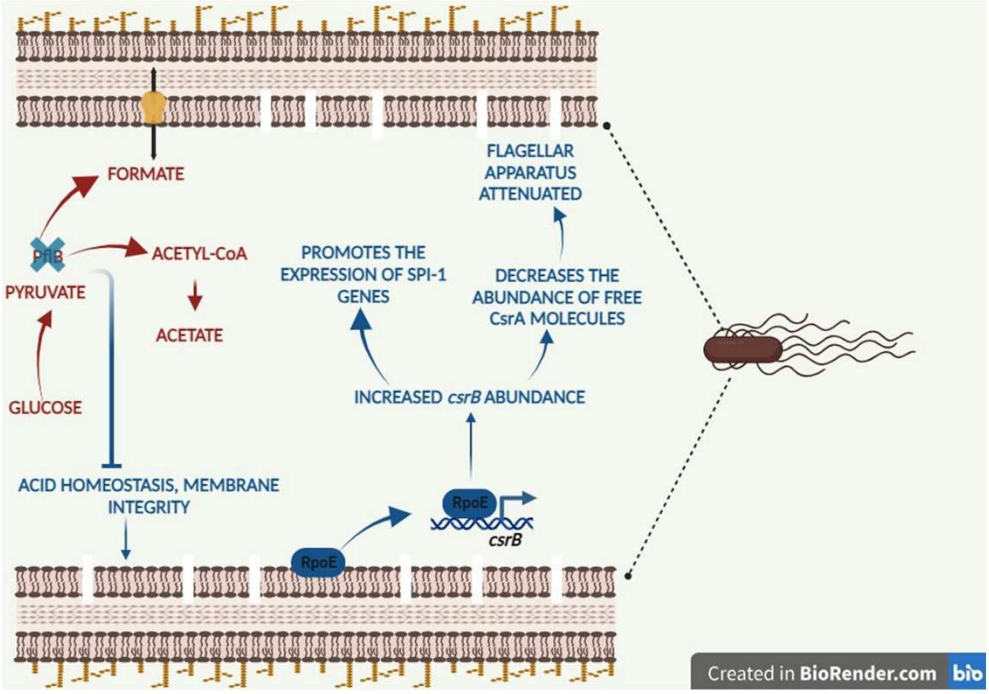

Figure 8

Figure 7: Regulation of flagellar machinery and SPI-1 apparatus by intracellular formate

Intracellular formate maintains the ipH of the cell. Perturbations in the formate pool bring about membrane depolarization, causing the migration of RpoE to csrB promoter. Overexpression of csrB upregulates the SPI-1 machinery and causes depletion of free CsrA molecules. The latter leads to a flagella deficient cell.

600

601 # STAR Methods

602 **Bacterial strains and plasmids**

603 The wild-type *Salmonella enterica* subspecies *enterica* serovar Typhimurium strain 14028S
604 used in this study was a kind gift from Professor Michael Hensel, Max Von Pettenkofer-
605 Institute for Hygiene und Medizinische Mikrobiologie, Germany. The knockout and
606 complement strains were generated for this study. The glycerol stocks of the bacterial strains
607 were stored in -80˚C and revived on fresh Luria-Bertani (LB) Agar (HiMedia) plates
608 supplemented with appropriate antibiotics (50 µg/ml Kanamycin, 50 µg/ml Ampicillin, 25
609 µg/ml Chloramphenicol) when required. A single colony was inoculated into a fresh LB tube
610 supplemented with antibiotics whenever required and incubated at 37˚C under shaking
611 conditions (170 rpm) to obtain an overnight culture of the bacterial strains. Strains harbouring
612 pKD46 plasmid were incubated overnight at 30˚C under shaking conditions (170 rpm). A
613 complete list of bacterial strains and plasmids used in this study has been given below in Table
614 A.

615 **Table A:**

Strains/ plasmids	**Characteristics**	**Source/ Information**
Salmonella enterica subspecies *enterica* serovar Typhimurium strain 14028S	Wild type (WT)	Gift from Prof. M. Hensel
S. Typhimurium *ΔfocA*	Chl^R	This study
S. Typhimurium *ΔpflB*	Kan^R	This study
S. Typhimurium *ΔpflB*/pQE60	Kan^R, Amp^R	This study

S. Typhimurium *ΔpflB*/pQE60: *pflB*	Kan^R, Amp^R	This study
S. Typhimurium *ΔfocAΔpflB*	Kan^R, Chl^R	This study
S. Typhimurium *ΔfliC*	Kan^R	Laboratory stock
S. Typhimurium/pQE60: *csrA*	Amp^R	This study
S. Typhimurium *ΔpflB*/pQE60: *csrA*	Kan^R, Amp^R	This study
S. Typhimurium *ΔpflBΔrpoE*	Kan^R, Chl^R	This study
S. Typhimurium *ΔpflBΔsirA*	Kan^R, Chl^R	This study
pKD4	Plasmid with FRT flanked Kanamycin-resistant cassette	
pKD3	Plasmid with FRT flanked Chloramphenicol-resistant cassette	
pKD46	Plasmid expressing λ-red recombinase system, Amp^R	
pQE60 vector	Low copy number plasmid, Amp^R	Laboratory stock
pBAD:pHuji	Amp^R	Addgene
pFPV:mCherry	Amp^R	Laboratory stock

616

617 **Construction of the knockout strains of *Salmonella***

618 The knockout strains of *Salmonella* were generated by following the one-step chromosomal
619 gene inactivation technique as described by Datsenko and Wanner (21). Briefly, STM (WT)
620 was transformed with pKD46 plasmid expressing λ-red recombinase system under Arabinose-
621 inducible plasmid. The transformed cells were selected in LB plates supplemented with 50
622 µg/ml Ampicillin. For generating the knockout strains, a single colony of STM (WT)/ pKD46
623 was inoculated in a fresh LB tube supplemented with 50 µg/ml Ampicillin and 50 mM
624 Arabinose and incubated at 30˚C overnight under shaking conditions (170 rpm). The overnight
625 culture was sub-cultured in fresh LB tubes and incubated for 2.5 h under similar conditions to
626 obtain an OD_{600} of 0.35-0.4. Electrocompetent STM (WT)/pKD46 was prepared by washing
627 the bacterial pellet with chilled and autoclaved MilliQ and 10% Glycerol. Kanamycin (Kan^R,
628 1.5 kb cassette) resistance cassette and Chloramphenicol (Chl^R, 1.1 kb cassette) were amplified
629 from pKD4 and pKD3 plasmids using the knockout primers. The amplified Kan^R and Chl^R
630 cassettes were electroporated in STM (WT)/pKD46. The transformed cells were selected on
631 LB Agar plate using appropriate antibiotics (Kanamycin, Chloramphenicol). The knockout
632 colonies were confirmed by using gene-specific intragenic primers, knockout confirmatory
633 primers, and antibiotic-cassette specific primers.

634 The double knockout strains were generated by briefly modifying the one-step chromosomal
635 gene inactivation method as described by Datsenko and Wanner. Briefly, STM *ΔpflB* was
636 transformed with pKD46 plasmid. Overnight culture of the transformed strain was sub-cultured
637 into fresh LB tube supplemented with 50 mM Arabinose and 50 µg/ml Ampicillin and
638 incubated for 2.5 h at 30˚C (170 rpm) till it reached an OD_{600} of 0.3-0.4. Chloramphenicol gene
639 cassette (1.1 kb) flanked with homologous regions of *focA* was electroporated into
640 electrocompetent STM *ΔpflB*/pKD46 to generate STM *ΔfocAΔpflB*. The double-knockout
641 strains were selected on LB Agar supplemented with Kanamycin (50 µg/ml) and
642 Chloramphenicol (25 µg/ml). The double knockout colonies were further confirmed with

643 knockout confirmatory and gene specific intragenic primers. Primers used for knockout
644 generation have been enlisted in Table B.

645

646 **Construction of complemented and overexpression strains of *Salmonella***

647 The genes *pflB* and *csrA* were amplified from the genomic DNA of the wild-type *Salmonella*
648 by using their respective cloning primers. The colony PCR products and the empty pQE60
649 cloning vector were subjected to restriction digestion with BamHI-HF (NEB) and HindIII-HF
650 (NEB) at 37˚C for 1 hour. The double-digested insert and vector were further purified and
651 subjected to ligation by T4 DNA Ligase (NEB) at 16˚C overnight. The ligated product was
652 further transformed into *Escherichia coli* TG1 by heat shock method. Cloning was confirmed
653 by double digestion of the recombinant plasmid. The recombinant plasmid was transformed
654 into *Salmonella* strains to generate complemented and overexpression strains. Primers used for
655 complement strain generation have been enlisted in Table B.

656

657 **RNA Isolation and RT-qPCR**

658 Logarithmic culture of bacterial cells was centrifuged at 6,000 rpm at 4˚C and the pellet was
659 resuspended in TRIzol reagent. It was stored at -80˚C till further use. RNA was isolated from
660 the lysed supernatants by using the chloroform-isopropanol method. The RNA pellet was
661 washed using 70% Ethanol and it was resuspended in 30 µl of DEPC treated MilliQ. RNA
662 concentration was measured in NanoDrop (Thermo Fischer Scientific) and the quality was
663 assessed on a 2% agarose gel. Following this, 2 µg RNA was subjected to DNase treatment in
664 presence of DNase TURBO (Thermo Fischer Scientific) at 37˚C for 30 mins. The DNase was
665 inactivated by addition of 5 mM Na_2EDTA (Thermo Fischer Scientific), followed by incubation
666 at 65˚C for 10 mins. The cDNA synthesis was performed using the PrimeScript RT reagent kit

667 of Takara (CAT RR037A), following the manufacturer's protocol. Quantitative Real Time PCR
668 was performed using TB Green RT-qPCR kit (Takara) in Quant 5 Real-Time PCR system.
669 Intragenic primers were used to study the expression of the genes. The gene expression level
670 was normalized with the expression of 16S rRNA. The primer sequences are mentioned in
671 Table B.

672

673 **TABLE B:**

PRIMER NAME	**SEQUENCE (5'-3')**
16S rRNA RT FP	GTGAGGTAACGGCTCACCAA
16S rRNA RT RP	TAACCGCAACACCTTCCTCC
hilA RT FP	GCCGGTGACCATTACGAAGA
hilA RT RP	AAGAGAGAAGCGGGTTGGTG
prgH RT FP	CGTTTTCAGGTGTTGCCAGG
prgH RT RP	TACGCGGCTCATCGAAATGA

flhD RT FP	CGCCTCGGTATCAACGAAGA
flhD RT RP	CACTTCATTGAGCAGACGCG
fliC RT FP	CTAAACAAACTGGGTGGCGC
fliC RT RP	GCACCCAGGTCAGAACGTAA
flgA RT FP	ATTATGTCGCCGTTGCC
flgA RT RP	TGACCTGTACTCGTTGC
flgK RT FP	AACCACCGATCAGTATC
flgK RT RP	TCGTCAGGTTATAGGTG
fliA RT FP	GCTGGATGAATTACGCA
fliA RT RP	CCACTCATCGTAAGAGA
motA RT FP	TTGCTGGCGTTGCTCTA
motA RT RP	GATGATCAGGCGCAGAT

csrB RT FP	CGTACAACGAAGCGAACGTC
csrB RT RP	TGTGACCTTACGGCCTGTTC
focA KO FP	ACACCGTAATTGCATAAAAGCCATGCGACTTACGGGCCTACATATGAATATCCTCCTTAG
focA KO RP	ATGCTCGTTACCACGCAGGTAAATGACCCAGTATGTCAACGTGTAGGCTGGAGCTGCTTC
pflB KO FP	ATGTCCGAGCTTAATGAAAAGTTAGCCACAGCCTGGGAACATATGAATATCCTCCTTAG
pflB KO RP	TACATGGTCTGCGTGAAGGTACGAGTAATAACGTCCTGCTGTGTAGGCTGGAGCTGCTTC
focA RT FP	CGGAAAGCCACATCAGTAAC
focA RT RP	ATCGGGGGTATCTGTTTCTC
pflB RT FP	ATAACGTCCTGCTGCTGTTC
pflB RT RP	ATGGTTACTTCCACCACGAA
pflB cloning FP	CGCGGATCCATGTCCGAGCTTAATGA

pflB cloning RP	CCCAAGCTTCAGTCAAACCCATTACA
rpoE KO FP	GGTTTGGGGAGACATTACCTCGGATGAGCGAGCAGTTACATATGAATATCCTCCTTAG
rpoE KO RP	CCTAATACCTTTTCCAGTATCCCGCTATCGTCAACGGTGTAGGCTGGAGCTGCTTC
sirA KO FP	CTATCAGTAGCGTTATCCCTATTCTGGAGATATTCCTTTGCATATGAATATCCTCCTTAG
sirA KO RP	ATACGATAGCGATAGCTGTTCACCGTTTTAGGACTGAGATGTGTAGGCTGGAGCTCTTC
csrA cloning FP	CGCGGATCCATGCTGATTCTGACTCG
csrA cloning RP	CCCAAGCTTTTAGTAACTGGACTGCTGG

674

675 **Eukaryotic cell lines and growth conditions**

676 The HeLa, Caco-2, HepG2, RAW 264.7 cell lines were maintained in Dulbecco's Modified
677 Eagle's Medium (DMEM, Sigma-Aldrich), supplemented with 10% Fetal Calf Serum (FCS,
678 Gibco) at 37˚C, in the presence of 5% CO_2.

679

680 **Gentamicin Protection Assay and Intracellular Cell Survival Assay**

681 Caco-2 and RAW 264.7 cells were seeded into tissue culture treated 24-well plates. For
682 infection in epithelial cell Caco-2, the overnight cultures of STM WT, STM *ΔpflB*, STM
683 *ΔpflB*/pQE60: *pflB*, and STM *ΔfocAΔpflB* were subcultured into fresh LB tubes supplemented
684 with or without 40 mM Sodium Formate (Sigma). For infection in the macrophage cell line
685 RAW 264.7, the overnight cultures of the bacterial strains were used. Both the cell lines were
686 infected at an MOI of 10. After centrifuging the cells at 1000 rpm for 10 mins, the cells were
687 incubated at 37˚C for 25 mins in the presence of 5% CO_2. The cells were then washed with 1X
688 Phosphate Buffer Saline (PBS) to remove the extracellular unadhered and loosely adhered
689 bacteria before addition of media containing 100 µg/ml of gentamicin. After incubation for 1
690 hour, the cells were washed with 1X PBS and were subjected to 25 µg/ml of gentamicin
691 treatment till the time of lysis. The cells were lysed at 2h and 16h post-infection with 0.1%
692 Triton X-100 and the lysates were plated on *Salmonella-Shigella* (SS) Agar along with the pre-
693 inoculum. The percent invasion and the fold proliferation were calculated using the following
694 formulae:

695 **Percent invasion/phagocytosis= [C.F.U at 2h/ C.F.U of Pre-Inoculum] *100**

696 **Fold proliferation= [C.F.U at 16h/ C.F.U of 2h]**

697

698 **Adhesion assay**

699 The adhesion assay was performed by modifying the previously reported protocol (97). Briefly,
700 Caco-2 cells were seeded into tissue culture treated 24-well plates. The 12h-old overnight
701 cultures of STM WT, STM *ΔpflB*, and STM *ΔfliC* were sub cultured into fresh LB tubes
702 supplemented with or without 40 mM Sodium Formate (Sigma). The cells were infected with
703 the logarithmic phase of these bacterial strains at an MOI of 10. The cells were centrifuged at
704 1000 rpm for 10 mins. Following this, the cells were incubated at 37˚C for 10 mins in the

705 presence of 5% CO_2. The cells were then washed with 1X Phosphate Buffer Saline (PBS) twice
706 to remove the extracellular unadhered and loosely adhered bacteria. The cells were lysed with
707 0.1% Triton X-100 and the lysates were plated on *Salmonella-Shigella* (SS) Agar along with
708 the pre-inoculum. The percent adhesion was calculated using the following formula:

709 **Percent adhesion= [C.F.U at 10 mins Post Infection/ C.F.U of Pre-Inoculum] *100**

710

711 **TEM**

712 Transmission Electron Microscopy was performed by modifying the protocol by Marathe *et al*
713 (98). Briefly, overnight cultures of STM WT, STM *ΔpflB*, STM *ΔfocA*, STM *ΔfocAΔpflB*, STM
714 WT/*csrA,* STM *ΔpflB/csrA,* STM *ΔrpoE*, and STM *ΔpflBΔrpoE* were sub cultured (1:100) (+/-
715 F) into fresh LB tubes and incubated at 37℃ for 2.5- 3 hours under shaking conditions. Next,
716 the samples were washed twice with 1X PBS and finally resuspended in 50 µl of 1X PBS. 5 µl
717 of this sample was placed on glow-discharged Cu-grid followed by air-drying. The bacteria
718 were negatively stained with 1% uranyl acetate. The samples were air-dried followed by
719 imaging with Transmission Electron Microscopy (JEM-100 CX II; JEOL).

720

721 **Confocal Microscopy**

722 Confocal Microscopy was performed by modifying the protocol by Marathe *et al* (98). Briefly,
723 12h old stationary phase cultures of STM WT, STM *ΔpflB*, STM *ΔfocAΔpflB*, STM WT/*csrA,*
724 STM *ΔpflB/csrA,* STM *ΔrpoE*, STM *ΔpflBΔrpoE,* (+/-F) were subcultured (1:100) into fresh
725 LB tubes and incubated at 37℃ for 2.5- 3 hours under shaking conditions till it reached the
726 logarithmic phase. Following this, 100 µl of the log phase culture was spotted onto sterile
727 coverslips and were air-dried overnight. Once the samples were completely dried, 3.5%

728 Paraformaldehyde (PFA) was added to the coverslips to fix the samples. The PFA was washed
729 away by using 1X PBS and the Rabbit raised Anti-Fli primary antibody (1:100 dilution in 2.5%
730 BSA solution, Difco) was used to stain the fixed samples for 3h at room temperature. After
731 washing away the primary antibody with 1X PBS, the samples were incubated with the
732 secondary antibody Alexa-488 conjugated Anti-Rabbit antibody (Sigma) for 45 mins at room
733 temperature. Immediately prior to mounting of the coverslip onto a clean glass slide, the
734 samples were stained with 4`,6-diamidino-2-phenylindole (DAPI) for 5 mins. Transparent nail
735 paint was used to seal the coverslips. All the images were obtained with Zeiss 880 and were
736 analysed using Zeiss ZEN Black 2012 Software.

737

738 **Gas Chromatography Mass Spectrometry**

739 GC-MS was performed by modifying the protocol by Hughes *et al* (99). Briefly, overnight
740 cultures of STM WT, STM *ΔpflB*, STM *ΔfocA*, STM *ΔfocAΔpflB* were sub cultured (1:100)
741 into 100 ml of LB Broth. After 2.5-3h of incubation at 37˚C under shaking conditions, 50 ml
742 of the individual cultures was centrifuged at 6,000 rpm for 10 mins. The pellet was washed
743 twice with 1X PBS to remove the remnants of the media. Finally, the pellet was resuspended
744 in 1 ml of 1X PBS, and the suspension was sonicated to lyse the bacterial cells. The cell debris
745 were removed by centrifugation. Prior to sonication, the CFU in the pellet had been recorded
746 by plating.

747 Sodium formate (Sigma) was used as an external standard. External standards and biological
748 samples were derivatized prior to the Mass Spectrometry. 2 M hydrochloric acid was added in
749 a 1:1 ratio to the samples to protonate formate. Liquid-liquid extraction was done which
750 extracted formic acid into ethyl acetate (Sigma-Aldrich). To remove any remaining water, the
751 ethyl acetate extract was passed through a column of anhydrous sodium sulfate (Sigma-

752 Aldrich). The ethyl acetate extract of formic acid was then incubated at 80 ºC for 1 h with the
753 derivatization reagent N, O-Bis(trimethylsilyl)trifluoro acetamide (Sigma Aldrich) with 1%
754 Chlorotrimethylsilane (Fluka). The derivatized samples were then transferred to autosampler
755 vials for analysis by Gas Chromatography Mass Spectrometry (Agilent technologies, 7890A
756 GC, 5975C MS). The injection temperature was set to 200 °C and the injection split ratio was
757 1:40 with an injection volume of 1 µL. The oven temperature set to start at 40 °C for 4 min,
758 with an increase to 120 °C at 5 °C per min and to 200 °C at 25 °C per min with a final hold at
759 this temperature for 3 min. Helium carrier gas had a flow rate of 1.2mL/min with constant flow
760 mode. A 30 m × 0.25 mm × 0.40 µm DB-624 column from Agilent was used. The interface
761 temperature set to 220 °C. The electron impact ion source temperature was at 230 °C, with an
762 ionization energy of 70 eV and 1235EM volts. For qualitative experiments, selected ion
763 monitoring (single quadrupole mode) of 103 m/z scan had been performed. The retention time
764 for formate and deuterated formate was 5.9 min. The target and reference (qualifier) ions for
765 formate were m/z = 103 and m/z = 75, respectively. The formate concentration of each sample
766 was interpolated from a standard curve with the known standards. It was normalized with the
767 CFU values of each sample to obtain the intracellular formate concentration/CFU.

768 To determine the formate transportation into the cell, we sub cultured overnight cultures of
769 STM WT, STM *ΔpflB*, STM *ΔfocA*, STM *ΔfocAΔpflB* into fresh LB tubes. During the
770 subculture, Sodium Formate was supplemented into each tube to maintain a concentration of
771 1M. Post 2.5-3h of incubation at 37˚C under shaking conditions, the bacterial cells were
772 removed from the media by centrifuging the culture twice at 6,000 rpm for 10 mins. A 2 µm
773 filter was used to remove any other bacterial cells left in the spent media. Following this, similar
774 protocol as mentioned above was used to quantify the residual formate in the spent media. It
775 was compared to the media where bacterial cells had not been sub cultured.

776

777 **Bisbenzimide Assay**

778 Bisbenzimide assay was performed by modifying the protocol by Roy Chowdhury *et al* (100).
779 Briefly, overnight cultures of STM WT, STM *ΔpflB*, STM *ΔfliC* were subcultured into fresh
780 LB tubes(+/-F). Logarithmic phase cultures of each condition was taken and the OD_{600} was
781 adjusted to 0.1. To 180 µl of this bacterial suspension, 20 µl of Bisbenzimide dye (10µg/ml)
782 was added. It was incubated at 37˚C for 10 mins. The intracellular DNA-bound bisbenzimide
783 was quantified in a TECAN 96 well microplate reader using a 346 nm excitation and 460 nm
784 emission filter.

785

786 **Staining with $DiBAC_4$**

787 Bisbenzimide assay was performed by modifying the protocol by Roy Chowdhury *et al* (101).
788 Membrane potential or membrane porosity was quantified by using a membrane potential
789 sensitive fluorescent dye bis-(1,3-dibutyl barbituric acid)- trimethylene oxonol (Invitrogen).
790 For this purpose, overnight culture of STM WT, STM *ΔpflB*, STM *ΔfliC* was subcultured with
791 or without the supplementation of 40 mM Sodium Formate (Sigma). Around 4.5*107 cells of
792 the logarithmic phase culture were incubated with 1 µg/ml of DiBAC4 dye at 37˚C for 30 mins.
793 The percent $DiBAC_4$-positive cells and the Median Fluorescence Intensity (MFI) of $DiBAC_4$
794 was determined by flow cytometry (BD FACSVerse by BD Biosciences-US).

795

796 **BCECF-AM Staining**

797 Bisbenzimide assay was performed by modifying the protocol by Roy Chowdhury *et al* (100).
798 The acidification of the cytosol with the change in pH of extracellular conditions was
799 detrimental determined using a cell-permeable dual excitation ratiometric dye 2',7'-Bis-(2-

800 Carboxyethyl)-5- (and-6)-Carboxyfluorescein, Acetoxymethyl Ester (BCECF-AM). Briefly,
801 the logarithmic phase cultures of STM WT, STM *ΔpflB* (+/-F) were resuspended in buffers of
802 different pH (5,5.5,6,7). They were incubated for 2 hours at 37˚C prior to addition of 1 mg/ml
803 BCECF-AM to make a final concentration of 20 µM. The cells were incubated with the dye
804 for 30 minutes. Post-incubation, the cells were analyzed by flow cytometry (BD FACSVerse
805 by BD Biosciences, US) with 488 nm and 405 nm excitation and 535 nm excitation channels.
806 The MFI of the bacterial cells at 488 nm and 405 nm was obtained from BD FACSuite software
807 and the ratio of 488/405 was utilised to determine the cytosolic acidification in response to
808 changing pH conditions.

809

810 **Intracellular pH measurement by pHuji plasmid**

811 STM WT and STM *ΔpflB* were transformed with the plasmid pBAD:pHuji (Plasmid #61555)
812 that encodes a pH sensitive red fluorescent protein pHuji (102, 103). The logarithmic cultures
813 of STM WT/pBAD:pHuji and STM *ΔpflB*/pBAD:pHuji (+/-F) were incubated in phosphate
814 buffers of pH 5,6,7,8,9 in presence of 40 µM Sodium Benzoate to equilibrate the intracellular
815 pH with the extracellular one. The resultant fluorescent intensity was plotted as a function of
816 pH and was fitted to obtain a standard curve. The fluorescence values obtained from LB-grown
817 cultures of the bacterial cells (+/- F) was interpolated in the standard curve to obtain then
818 intracellular pH of the bacterial cells *in-vitro*.

819

820 **Ethics statement for Animal Experiments**

821 All the animal experiments have been approved by the Institutional Animal Ethics Clearance
822 Committee (IAEC), Indian Institute of Science, Bangalore. The registration number is
823 48/1999/CPCSEA. The guidelines formulated by the Committee for the Purpose of Control

824 and Supervision of Experiments on Animals (CPCSEA) were strictly followed. The ethical
825 clearance number for this study is CAF/Ethics/853/2021.

826

827 **Mice Survival Assay**

828 6-8 weeks old male C57BL/6 mice and Balb/c mice were acquired from the specific-pathogen
829 free conditions of Central Animal Facility, IISc. To draw a comparison between the mortality
830 rate of WT and mutant strains, the mice (n=10) were orally gavaged with 10^8 cells from the
831 stationary phase culture of each. After infection, the mice were monitored every day for
832 survival, and the data was represented as percent survival.

833

834 **Determination of bacterial burden in different organs**

835 To understand the organ burden of the WT and mutant strain post infection in mice, 10^7 cells
836 from the overnight culture of the bacterial strains were orally gavaged into 6-8 weeks old
837 C57BL/6 mice. 5 days post infection, the mice were ethically euthanized, and the liver, spleen,
838 and brain were acquired. The organs were homogenized, and appropriate dilutions of the
839 homogenate was plated on *Salmonella-Shigella* (SS Agar). The data was represented was
840 $\log_{10}$CFU/gm-wt.

841

842 **Invasion Assay in mice**

843 Invasion assay in mice was performed by modifying the protocol by Chandra *et al* (104).
844 Briefly, 10^7 cells from the overnight culture of the bacterial cells were orally gavaged into 6-8
845 weeks old male C57BL/6 mice. 6 hours post infection, the mice were ethically euthanized, and
846 the intestine was acquired. It was homogenized, and appropriate dilutions of the homogenate

was plated on *Salmonella-Shigella* (SS Agar). Corresponding fecal matter was also collected and it was also plated post homogenization. The data was represented was $\log_{10}$CFU/gm-wt.

Intraperitoneal infection of mice

Intraperitoneal infection of mice was performed with 10^3 CFU from the overnight cultures of WT and mutant strains. 2 days post infection, the mice were ethically euthanized, and the liver, and the spleen were obtained. The organ burden of the bacterial strains was determined by the same protocol as above.

Statistical Analysis

Each experiment has been repeated 1 to 8 times independently as mentioned in the figure legends. The statistical analyses were performed by two-way Student's t-test or two-way ANOVA multiple comparison test as denoted in the figure legends. The data obtained from the mice experiments were analyzed using the Mann-Whitney *U* test. The *p* values below 0.05 were considered significant. The results are indicated as Mean ± SD or Mean ± SEM as mentioned in the figure legends. All the data were plotted and analysed using GraphPad Prism 8.4.2.

References

1. Galanis E, Lo Fo Wong DM, Patrick ME, Binsztein N, Cieslik A, Chalermchikit T, et al. Web-based surveillance and global Salmonella distribution, 2000-2002. Emerg Infect Dis. 2006;12(3):381-8.
2. Collaborators GBDCoD. Global, regional, and national age-sex-specific mortality for 282 causes of death in 195 countries and territories, 1980-2017: a systematic analysis for the Global Burden of Disease Study 2017. Lancet. 2018;392(10159):1736-88.

3. DALYs GBD, Collaborators H. Global, regional, and national disability-adjusted life-years (DALYs) for 359 diseases and injuries and healthy life expectancy (HALE) for 195 countries and territories, 1990-2017: a systematic analysis for the Global Burden of Disease Study 2017. Lancet. 2018;392(10159):1859-922.
4. Disease GBD, Injury I, Prevalence C. Global, regional, and national incidence, prevalence, and years lived with disability for 354 diseases and injuries for 195 countries and territories, 1990-2017: a systematic analysis for the Global Burden of Disease Study 2017. Lancet. 2018;392(10159):1789-858.
5. Crump JA, Sjolund-Karlsson M, Gordon MA, Parry CM. Epidemiology, Clinical Presentation, Laboratory Diagnosis, Antimicrobial Resistance, and Antimicrobial Management of Invasive Salmonella Infections. Clin Microbiol Rev. 2015;28(4):901-37.
6. Maslowski KM, Vieira AT, Ng A, Kranich J, Sierro F, Yu D, et al. Regulation of inflammatory responses by gut microbiota and chemoattractant receptor GPR43. Nature. 2009;461(7268):1282-6.
7. Tan J, McKenzie C, Potamitis M, Thorburn AN, Mackay CR, Macia L. The role of short-chain fatty acids in health and disease. Advances in immunology. 2014;121:91-119.
8. Thorburn AN, Macia L, Mackay CR. Diet, metabolites, and "western-lifestyle" inflammatory diseases. Immunity. 2014;40(6):833-42.
9. Huffnagle GB. Increase in dietary fiber dampens allergic responses in the lung. Nat Med. 2014;20(2):120-1.
10. Machado MG, Sencio V, Trottein F. Short-Chain Fatty Acids as a Potential Treatment for Infections: a Closer Look at the Lungs. Infect Immun. 2021;89(9):e0018821.
11. Jacobson A, Lam L, Rajendram M, Tamburini F, Honeycutt J, Pham T, et al. A Gut Commensal-Produced Metabolite Mediates Colonization Resistance to Salmonella Infection. Cell Host Microbe. 2018;24(2):296-307 e7.
12. Boyen F, Haesebrouck F, Vanparys A, Volf J, Mahu M, Van Immerseel F, et al. Coated fatty acids alter virulence properties of Salmonella Typhimurium and decrease intestinal colonization of pigs. Vet Microbiol. 2008;132(3-4):319-27.
13. Gantois I, Ducatelle R, Pasmans F, Haesebrouck F, Hautefort I, Thompson A, et al. Butyrate specifically down-regulates salmonella pathogenicity island 1 gene expression. Appl Environ Microbiol. 2006;72(1):946-9.
14. Lawhon SD, Maurer R, Suyemoto M, Altier C. Intestinal short-chain fatty acids alter Salmonella typhimurium invasion gene expression and virulence through BarA/SirA. Mol Microbiol. 2002;46(5):1451-64.
15. Lamas A, Regal P, Vázquez B, Cepeda A, Franco CM. Short chain fatty acids commonly produced by gut microbiota influence Salmonella enterica motility, biofilm formation, and gene expression. Antibiotics. 2019;8(4):265.
16. Amrutha B, Sundar K, Shetty PH. Effect of organic acids on biofilm formation and quorum signaling of pathogens from fresh fruits and vegetables. Microb Pathog. 2017;111:156-62.
17. Huang Y, Suyemoto M, Garner CD, Cicconi KM, Altier C. Formate acts as a diffusible signal to induce Salmonella invasion. J Bacteriol. 2008;190(12):4233-41.
18. Chowdhury R, Pavinski Bitar PD, Chapman HM, Altier C. Salmonella Invasion Is Controlled by Competition among Intestinal Chemical Signals. mBio. 2023;14(2):e0001223.
19. Winter MG, Hughes ER, Muramatsu MK, Jimenez AG, Chanin RB, Spiga L, et al. Formate oxidation in the intestinal mucus layer enhances fitness of Salmonella enterica serovar Typhimurium. mBio. 2023;14(4):e0092123.
20. Abernathy J, Corkill C, Hinojosa C, Li X, Zhou H. Deletions in the pyruvate pathway of Salmonella Typhimurium alter SPI1-mediated gene expression and infectivity. J Anim Sci Biotechnol. 2013;4(1):5.
21. Datsenko KA, Wanner BL. One-step inactivation of chromosomal genes in Escherichia coli K-12 using PCR products. Proc Natl Acad Sci U S A. 2000;97(12):6640-5.
22. Lu W, Du J, Wacker T, Gerbig-Smentek E, Andrade SL, Einsle O. pH-dependent gating in a FocA formate channel. Science. 2011;332(6027):352-4.

923 23. Dong R, Liang Y, He S, Cui Y, Shi C, He Y, et al. DsrA Modulates Central Carbon Metabolism and
924 Redox Balance by Directly Repressing pflB Expression in Salmonella Typhimurium. Microbiol Spectr.
925 2022;10(1):e0152221.
926 24. Parker CT, Guard-Petter J. Contribution of flagella and invasion proteins to pathogenesis of
927 Salmonella enterica serovar enteritidis in chicks. FEMS Microbiol Lett. 2001;204(2):287-91.
928 25. Haiko J, Westerlund-Wikstrom B. The role of the bacterial flagellum in adhesion and
929 virulence. Biology (Basel). 2013;2(4):1242-67.
930 26. Rossez Y, Wolfson EB, Holmes A, Gally DL, Holden NJ. Bacterial flagella: twist and stick, or
931 dodge across the kingdoms. PLoS Pathog. 2015;11(1):e1004483.
932 27. Gut AM, Vasiljevic T, Yeager T, Donkor ON. Salmonella infection - prevention and treatment
933 by antibiotics and probiotic yeasts: a review. Microbiology (Reading). 2018;164(11):1327-44.
934 28. Agbor TA, McCormick BA. Salmonella effectors: important players modulating host cell
935 function during infection. Cell Microbiol. 2011;13(12):1858-69.
936 29. Finlay BB, Ruschkowski S, Dedhar S. Cytoskeletal rearrangements accompanying salmonella
937 entry into epithelial cells. J Cell Sci. 1991;99 (Pt 2):283-96.
938 30. Zhou D, Galan J. Salmonella entry into host cells: the work in concert of type III secreted
939 effector proteins. Microbes Infect. 2001;3(14-15):1293-8.
940 31. Kammel M, Pinske C, Sawers RG. FocA and its central role in fine-tuning pH homeostasis of
941 enterobacterial formate metabolism. Microbiology (Reading). 2022;168(10).
942 32. Suppmann B, Sawers G. Isolation and characterization of hypophosphite-resistant mutants of
943 Escherichia coli: identification of the FocA protein, encoded by the pfl operon, as a putative formate
944 transporter. Molecular Microbiology. 1994;11(5):965-82.
945 33. Kammel M, Sawers RG. The FocA channel functions to maintain intracellular formate
946 homeostasis during Escherichia coli fermentation. Microbiology. 2022;168(4).
947 34. Beyer L, Doberenz C, Falke D, Hunger D, Suppmann B, Sawers RG. Coordination of FocA and
948 pyruvate formate-lyase synthesis in Escherichia coli demonstrates preferential translocation of
949 formate over other mixed-acid fermentation products. J Bacteriol. 2013;195(7):1428-35.
950 35. Wiechert M, Beitz E. Mechanism of formate-nitrite transporters by dielectric shift of
951 substrate acidity. EMBO J. 2017;36(7):949-58.
952 36. Lyu M, Su CC, Kazura JW, Yu EW. Structural basis of transport and inhibition of the
953 Plasmodium falciparum transporter PfFNT. EMBO reports. 2021;22(3):e51628.
954 37. Helmstetter F, Arnold P, Hoger B, Petersen LM, Beitz E. Formate-nitrite transporters carrying
955 nonprotonatable amide amino acids instead of a central histidine maintain pH-dependent transport.
956 J Biol Chem. 2019;294(2):623-31.
957 38. Minamino T, Imae Y, Oosawa F, Kobayashi Y, Oosawa K. Effect of intracellular pH on rotational
958 speed of bacterial flagellar motors. J Bacteriol. 2003;185(4):1190-4.
959 39. Putnam RW. Chapter 17 - Intracellular pH Regulation. In: Sperelakis N, editor. Cell Physiology
960 Source Book (Fourth Edition). San Diego: Academic Press; 2012. p. 303-21.
961 40. Kutsukake K, Ide N. Transcriptional analysis of the flgK and fliD operons of Salmonella
962 typhimurium which encode flagellar hook-associated proteins. Mol Gen Genet. 1995;247(3):275-81.
963 41. Gillen KL, Hughes KT. Transcription from two promoters and autoregulation contribute to the
964 control of expression of the Salmonella typhimurium flagellar regulatory gene flgM. J Bacteriol.
965 1993;175(21):7006-15.
966 42. Ikebe T, Iyoda S, Kutsukake K. Structure and expression of the fliA operon of Salmonella
967 typhimurium. Microbiology (Reading). 1999;145 (Pt 6):1389-96.
968 43. Ohnishi K, Kutsukake K, Suzuki H, Iino T. Gene fliA encodes an alternative sigma factor
969 specific for flagellar operons in Salmonella typhimurium. Mol Gen Genet. 1990;221(2):139-47.
970 44. Karlinsey JE, Tanaka S, Bettenworth V, Yamaguchi S, Boos W, Aizawa SI, et al. Completion of
971 the hook-basal body complex of the Salmonella typhimurium flagellum is coupled to FlgM secretion
972 and fliC transcription. Mol Microbiol. 2000;37(5):1220-31.

973 45. Ohnishi K, Kutsukake K, Suzuki H, Lino T. A novel transcriptional regulation mechanism in the
974 flagellar regulon of Salmonella typhimurium: an antisigma factor inhibits the activity of the flagellum-
975 specific sigma factor, sigma F. Mol Microbiol. 1992;6(21):3149-57.
976 46. Fraser GM, Hirano T, Ferris HU, Devgan LL, Kihara M, Macnab RM. Substrate specificity of
977 type III flagellar protein export in Salmonella is controlled by subdomain interactions in FlhB. Mol
978 Microbiol. 2003;48(4):1043-57.
979 47. Hirano T, Minamino T, Namba K, Macnab RM. Substrate specificity classes and the
980 recognition signal for Salmonella type III flagellar export. J Bacteriol. 2003;185(8):2485-92.
981 48. Frye J, Karlinsey JE, Felise HR, Marzolf B, Dowidar N, McClelland M, et al. Identification of
982 new flagellar genes of Salmonella enterica serovar Typhimurium. J Bacteriol. 2006;188(6):2233-43.
983 49. Kutsukake K. Autogenous and global control of the flagellar master operon, flhD, in
984 Salmonella typhimurium. Mol Gen Genet. 1997;254(4):440-8.
985 50. Tanabe Y, Wada T, Ono K, Abo T, Kutsukake K. The transcript from the sigma(28)-dependent
986 promoter is translationally inert in the expression of the sigma(28)-encoding gene fliA in the fliAZ
987 operon of Salmonella enterica serovar Typhimurium. J Bacteriol. 2011;193(22):6132-41.
988 51. Ko M, Park C. H-NS-Dependent regulation of flagellar synthesis is mediated by a LysR family
989 protein. J Bacteriol. 2000;182(16):4670-2.
990 52. Vakulskas CA, Potts AH, Babitzke P, Ahmer BM, Romeo T. Regulation of bacterial virulence by
991 Csr (Rsm) systems. Microbiol Mol Biol Rev. 2015;79(2):193-224.
992 53. Romeo T. Global regulation by the small RNA-binding protein CsrA and the non-coding RNA
993 molecule CsrB. Mol Microbiol. 1998;29(6):1321-30.
994 54. Yakhnin AV, Baker CS, Vakulskas CA, Yakhnin H, Berezin I, Romeo T, et al. CsrA activates flhDC
995 expression by protecting flhDC mRNA from RNase E-mediated cleavage. Mol Microbiol.
996 2013;87(4):851-66.
997 55. Liu MY, Gui G, Wei B, Preston JF, 3rd, Oakford L, Yuksel U, et al. The RNA molecule CsrB binds
998 to the global regulatory protein CsrA and antagonizes its activity in Escherichia coli. J Biol Chem.
999 1997;272(28):17502-10.
1000 56. Weilbacher T, Suzuki K, Dubey AK, Wang X, Gudapaty S, Morozov I, et al. A novel sRNA
1001 component of the carbon storage regulatory system of Escherichia coli. Mol Microbiol.
1002 2003;48(3):657-70.
1003 57. Dubey AK, Baker CS, Romeo T, Babitzke P. RNA sequence and secondary structure participate
1004 in high-affinity CsrA-RNA interaction. RNA. 2005;11(10):1579-87.
1005 58. Altier C, Suyemoto M, Lawhon SD. Regulation of Salmonella enterica serovar typhimurium
1006 invasion genes by csrA. Infect Immun. 2000;68(12):6790-7.
1007 59. Lawhon SD, Frye JG, Suyemoto M, Porwollik S, McClelland M, Altier C. Global regulation by
1008 CsrA in Salmonella typhimurium. Mol Microbiol. 2003;48(6):1633-45.
1009 60. Suzuki K, Wang X, Weilbacher T, Pernestig AK, Melefors O, Georgellis D, et al. Regulatory
1010 circuitry of the CsrA/CsrB and BarA/UvrY systems of Escherichia coli. J Bacteriol. 2002;184(18):5130-
1011 40.
1012 61. Suzuki K, Wang X, Weilbacher T, Pernestig A-K, Melefors O, Georgellis D, et al. Regulatory
1013 circuitry of the CsrA/CsrB and BarA/UvrY systems of Escherichia coli. Journal of bacteriology.
1014 2002;184(18):5130-40.
1015 62. Teplitski M, Goodier RI, Ahmer BM. Pathways Leading from BarA/SirA to Motility
1016 andVirulence Gene Expression in Salmonella. Journal of bacteriology. 2003;185(24):7257-65.
1017 63. Weilbacher T, Suzuki K, Dubey AK, Wang X, Gudapaty S, Morozov I, et al. A novel sRNA
1018 component of the carbon storage regulatory system of Escherichia coli. Molecular microbiology.
1019 2003;48(3):657-70.
1020 64. Hayden JD, Ades SE. The extracytoplasmic stress factor, sigmaE, is required to maintain cell
1021 envelope integrity in Escherichia coli. PLoS One. 2008;3(2):e1573.

1022 65. Ahuja N, Korkin D, Chaba R, Cezairliyan BO, Sauer RT, Kim KK, et al. Analyzing the interaction
1023 of RseA and RseB, the two negative regulators of the sigmaE envelope stress response, using a
1024 combined bioinformatic and experimental strategy. J Biol Chem. 2009;284(8):5403-13.
1025 66. Lima S, Guo MS, Chaba R, Gross CA, Sauer RT. Dual molecular signals mediate the bacterial
1026 response to outer-membrane stress. Science. 2013;340(6134):837-41.
1027 67. De Las Penas A, Connolly L, Gross CA. The sigmaE-mediated response to extracytoplasmic
1028 stress in Escherichia coli is transduced by RseA and RseB, two negative regulators of sigmaE. Mol
1029 Microbiol. 1997;24(2):373-85.
1030 68. Missiakas D, Mayer MP, Lemaire M, Georgopoulos C, Raina S. Modulation of the Escherichia
1031 coli sigmaE (RpoE) heat-shock transcription-factor activity by the RseA, RseB and RseC proteins. Mol
1032 Microbiol. 1997;24(2):355-71.
1033 69. Campbell EA, Tupy JL, Gruber TM, Wang S, Sharp MM, Gross CA, et al. Crystal structure of
1034 Escherichia coli sigmaE with the cytoplasmic domain of its anti-sigma RseA. Mol Cell.
1035 2003;11(4):1067-78.
1036 70. Pannuri A, Vakulskas CA, Zere T, McGibbon LC, Edwards AN, Georgellis D, et al. Circuitry
1037 Linking the Catabolite Repression and Csr Global Regulatory Systems of Escherichia coli. J Bacteriol.
1038 2016;198(21):3000-15.
1039 71. Yakhnin H, Aichele R, Ades SE, Romeo T, Babitzke P. Circuitry Linking the Global Csr- and
1040 sigma(E)-Dependent Cell Envelope Stress Response Systems. J Bacteriol. 2017;199(23).
1041 72. Fabrega A, Vila J. Salmonella enterica serovar Typhimurium skills to succeed in the host:
1042 virulence and regulation. Clin Microbiol Rev. 2013;26(2):308-41.
1043 73. Kage H, Takaya A, Ohya M, Yamamoto T. Coordinated regulation of expression of Salmonella
1044 pathogenicity island 1 and flagellar type III secretion systems by ATP-dependent ClpXP protease. J
1045 Bacteriol. 2008;190(7):2470-8.
1046 74. Saini S, Brown JD, Aldridge PD, Rao CV. FliZ Is a posttranslational activator of FlhD4C2-
1047 dependent flagellar gene expression. J Bacteriol. 2008;190(14):4979-88.
1048 75. Singer HM, Kuhne C, Deditius JA, Hughes KT, Erhardt M. The Salmonella Spi1 virulence
1049 regulatory protein HilD directly activates transcription of the flagellar master operon flhDC. J
1050 Bacteriol. 2014;196(7):1448-57.
1051 76. Eichelberg K, Galan JE. The flagellar sigma factor FliA (sigma(28)) regulates the expression of
1052 Salmonella genes associated with the centisome 63 type III secretion system. Infect Immun.
1053 2000;68(5):2735-43.
1054 77. Iyoda S, Kamidoi T, Hirose K, Kutsukake K, Watanabe H. A flagellar gene fliZ regulates the
1055 expression of invasion genes and virulence phenotype in Salmonella enterica serovar Typhimurium.
1056 Microb Pathog. 2001;30(2):81-90.
1057 78. Lucas RL, Lostroh CP, DiRusso CC, Spector MP, Wanner BL, Lee CA. Multiple factors
1058 independently regulate hilA and invasion gene expression in Salmonella enterica serovar
1059 typhimurium. J Bacteriol. 2000;182(7):1872-82.
1060 79. Goodier RI, Ahmer BM. SirA orthologs affect both motility and virulence. J Bacteriol.
1061 2001;183(7):2249-58.
1062 80. Saleh DO, Horstmann JA, Giralt-Zuniga M, Weber W, Kaganovitch E, Durairaj AC, et al. SPI-1
1063 virulence gene expression modulates motility of Salmonella Typhimurium in a proton motive force-
1064 and adhesins-dependent manner. PLoS Pathog. 2023;19(6):e1011451.
1065 81. Gewirtz AT, Rao AS, Simon PO, Jr., Merlin D, Carnes D, Madara JL, et al. Salmonella
1066 typhimurium induces epithelial IL-8 expression via Ca(2+)-mediated activation of the NF-kappaB
1067 pathway. J Clin Invest. 2000;105(1):79-92.
1068 82. McSorley SJ, Cookson BT, Jenkins MK. Characterization of CD4+ T cell responses during
1069 natural infection with Salmonella typhimurium. J Immunol. 2000;164(2):986-93.
1070 83. Takahashi A, Wada A, Ogushi K, Maeda K, Kawahara T, Mawatari K, et al. Production of beta-
1071 defensin-2 by human colonic epithelial cells induced by Salmonella enteritidis flagella filament
1072 structural protein. FEBS Lett. 2001;508(3):484-8.

1073 84. Ellermeier CD, Slauch JM. RtsA and RtsB coordinately regulate expression of the invasion and
1074 flagellar genes in Salmonella enterica serovar Typhimurium. J Bacteriol. 2003;185(17):5096-108.
1075 85. Olsen JE, Hoegh-Andersen KH, Casadesus J, Rosenkranzt J, Chadfield MS, Thomsen LE. The
1076 role of flagella and chemotaxis genes in host pathogen interaction of the host adapted Salmonella
1077 enterica serovar Dublin compared to the broad host range serovar S. Typhimurium. BMC Microbiol.
1078 2013;13:67.
1079 86. Donohoe DR, Garge N, Zhang X, Sun W, O'Connell TM, Bunger MK, et al. The microbiome and
1080 butyrate regulate energy metabolism and autophagy in the mammalian colon. Cell Metab.
1081 2011;13(5):517-26.
1082 87. Levitt MD, Furne J, Springfield J, Suarez F, DeMaster E. Detoxification of hydrogen sulfide and
1083 methanethiol in the cecal mucosa. J Clin Invest. 1999;104(8):1107-14.
1084 88. Furne J, Springfield J, Koenig T, DeMaster E, Levitt MD. Oxidation of hydrogen sulfide and
1085 methanethiol to thiosulfate by rat tissues: a specialized function of the colonic mucosa. Biochem
1086 Pharmacol. 2001;62(2):255-9.
1087 89. Rivera-Chavez F, Zhang LF, Faber F, Lopez CA, Byndloss MX, Olsan EE, et al. Depletion of
1088 Butyrate-Producing Clostridia from the Gut Microbiota Drives an Aerobic Luminal Expansion of
1089 Salmonella. Cell Host Microbe. 2016;19(4):443-54.
1090 90. Kelly CJ, Zheng L, Campbell EL, Saeedi B, Scholz CC, Bayless AJ, et al. Crosstalk between
1091 Microbiota-Derived Short-Chain Fatty Acids and Intestinal Epithelial HIF Augments Tissue Barrier
1092 Function. Cell Host Microbe. 2015;17(5):662-71.
1093 91. Winter SE, Thiennimitr P, Winter MG, Butler BP, Huseby DL, Crawford RW, et al. Gut
1094 inflammation provides a respiratory electron acceptor for Salmonella. Nature. 2010;467(7314):426-9.
1095 92. Lopez CA, Winter SE, Rivera-Chavez F, Xavier MN, Poon V, Nuccio SP, et al. Phage-mediated
1096 acquisition of a type III secreted effector protein boosts growth of salmonella by nitrate respiration.
1097 mBio. 2012;3(3).
1098 93. Gillis CC, Hughes ER, Spiga L, Winter MG, Zhu W, Furtado de Carvalho T, et al. Dysbiosis-
1099 Associated Change in Host Metabolism Generates Lactate to Support Salmonella Growth. Cell Host
1100 Microbe. 2018;23(1):54-64 e6.
1101 94. Spiga L, Winter MG, Furtado de Carvalho T, Zhu W, Hughes ER, Gillis CC, et al. An Oxidative
1102 Central Metabolism Enables Salmonella to Utilize Microbiota-Derived Succinate. Cell Host Microbe.
1103 2017;22(3):291-301 e6.
1104 95. Faber F, Thiennimitr P, Spiga L, Byndloss MX, Litvak Y, Lawhon S, et al. Respiration of
1105 Microbiota-Derived 1,2-propanediol Drives Salmonella Expansion during Colitis. PLoS Pathog.
1106 2017;13(1):e1006129.
1107 96. Thiennimitr P, Winter SE, Winter MG, Xavier MN, Tolstikov V, Huseby DL, et al. Intestinal
1108 inflammation allows Salmonella to use ethanolamine to compete with the microbiota. Proc Natl Acad
1109 Sci U S A. 2011;108(42):17480-5.
1110 97. Gagnon M, Zihler Berner A, Chervet N, Chassard C, Lacroix C. Comparison of the Caco-2, HT-
1111 29 and the mucus-secreting HT29-MTX intestinal cell models to investigate Salmonella adhesion and
1112 invasion. J Microbiol Methods. 2013;94(3):274-9.
1113 98. Marathe SA, Balakrishnan A, Negi VD, Sakorey D, Chandra N, Chakravortty D. Curcumin
1114 Reduces the Motility of Salmonella enterica Serovar Typhimurium by Binding to the Flagella, Thereby
1115 Leading to Flagellar Fragility and Shedding. J Bacteriol. 2016;198(13):1798-811.
1116 99. Hughes ER, Winter MG, Duerkop BA, Spiga L, Furtado de Carvalho T, Zhu W, et al. Microbial
1117 Respiration and Formate Oxidation as Metabolic Signatures of Inflammation-Associated Dysbiosis.
1118 Cell Host Microbe. 2017;21(2):208-19.
1119 100. Roy Chowdhury A, Sah S, Varshney U, Chakravortty D. Salmonella Typhimurium outer
1120 membrane protein A (OmpA) renders protection from nitrosative stress of macrophages by
1121 maintaining the stability of bacterial outer membrane. PLoS Pathog. 2022;18(8):e1010708.

101. Chowdhury AR, Mukherjee D, Singh AK, Chakravortty D. Loss of outer membrane protein A (OmpA) impairs the survival of Salmonella Typhimurium by inducing membrane damage in the presence of ceftazidime and meropenem. J Antimicrob Chemother. 2022;77(12):3376-89.
102. Shen Y, Rosendale M, Campbell RE, Perrais D. pHuji, a pH-sensitive red fluorescent protein for imaging of exo- and endocytosis. J Cell Biol. 2014;207(3):419-32.
103. Hajra D, Yadav V, Singh A, Chakravortty D. SIRT1 and SIRT3 impact host mitochondrial function and host- Salmonella pH balance during infection. bioRxiv. 2023:2023.09.11.557159.
104. Chandra K, Roy Chowdhury A, Chatterjee R, Chakravortty D. GH18 family glycoside hydrolase Chitinase A of Salmonella enhances virulence by facilitating invasion and modulating host immune responses. PLoS Pathog. 2022;18(4):e1010407.